signaling is predominantly found within the subclass of glioblastomas with abnormal PDGFRα signaling (37). Finally, constitutively active PI3K mutations (*PIK3CA* and *PIK3R1*) occur mostly in clinical glioblastomas without *PDGFRA* aberrations (4). Consequently, our results strongly suggest SHP-2/*PTPN11* as a potential target for treatments of glioblastomas with *PDGFRA* overexpression.

Methods

Cell lines and reagents. Primary *Ink4a/Arf*$^{-/-}$ mAsts were derived and propagated as previously described (7). Human glioma cell lines LN444, LN443, LN-Z308, and LN319 were obtained from ATCC or from our own collection (38). Unless otherwise mentioned, all glioma cell lines and primary mAsts were routinely maintained in 5% CO_2 at 37°C, in DMEM (Invitrogen) containing 10% FBS (Hyclone), 100 U/ml penicillin, and 100 μg/ml streptomycin (Invitrogen).

Histology and IHC. Studies using human tissues were reviewed and approved by the Institutional Review Board involving Human Subjects of the University of Pittsburgh. The specimens were de-identified human tissues, and thus no informed consent was required. A total of 158 paraffin-embedded thin sections of primary human glioma specimens were used, including 87 WHO grade IV GBMs, 34 grade III anaplastic astrocytomas, anaplastic oligodendrogliomas, or anaplastic oligodendroastrocytomas, and 37 grade II oligodendrogliomas and diffuse astrocytomas. Thin sections of human glioma specimens and mouse brains with various tumors were analyzed by IHC using indicated (e.g., Figure 8 legend and Results) antibodies or a TUNEL staining kit as previously described (38, 39). Briefly, the 5-μm human tissue sections were deparaffinized in xylene, followed by rehydration in graded ethanol. After washing with TBS, the antigen was retrieved by boiling the sections in a citrate buffer (pH 6.0) twice for 5 minutes. For mouse brain tissues with various gliomas, 5-μm frozen sections were fixed in pre-chilled acetone at -20°C for 5 minutes, rinsed with PBS, and blocked by AquaBlock (East Coast Biologics Inc.) for 1 hour at room temperature. Afterward, various tissue sections were then incubated with a primary antibody overnight at 4°C and blocked by Peroxidase Blocking Reagent (DAKO) for 10 minutes, followed by incubation with a biotinylated secondary antibody for 30 minutes at room temperature. After washing in PBS, stained tissue sections were visualized by diaminobenzidine chromophore and H_2O_2, followed by hematoxylin counterstaining. Sections were then dehydrated by graded ethanol and mounted with Permount Solution (Fisher).

Soft agar colony formation assay. Colony formation assay in soft agar was performed as previously described (40). Briefly, approximately 5,000 cells were seeded in a 0.5% Noble Agar top layer with a bottom layer of 0.8% Noble Agar in each of the triplicate wells of a 24-well plate. Growth factor–reduced Matrigel (1 mg/ml) was added into the top layer with or without inhibitors as indicated in figure legends (e.g., Figure 7 legend) and described in Results. PDGF-A–expressing cells in 10% of total cells were included as a source of PDGF-A. DMEM containing 10% FBS was added 3 days after plating and changed every 3 days thereafter. Colonies were scored after 2–3 weeks using Olympus SZX12 stereomicroscope, and data were analyzed using GraphPad Software.

Mouse glioma xenografts, IP, IB, tissue image analyses and quantifications, and siRNA. Experiments of mouse glioma xenografts, IP, IB, tissue imaging and analyses, and siRNA knockdown were performed as previously described (39). For details, see Supplemental Experimental Procedures.

Statistics. One-way ANOVA or an unpaired, 2-tailed Student's *t* test followed by Newman-Keuls post-test was performed using GraphPad Prism software. A *P* value of 0.05 or less was considered statistically significant.

Acknowledgments

We would like to thank Carl-Henrik Heldin at Uppsala University for PDGFRα and PDGF-A cDNAs, Russell O. Pieper at University of California San Francisco for pMXI-*gfp* retroviral vector, Lynda Chin at Dana-Farber Cancer Institute for the cDNA of p16INK4a, Yi Zheng at Cincinnati Children's Hospital Medical Center for cDNA of p19ARF, Tao Cheng at University of Pittsburgh for pMSCV retroviral vectors, and N. Balass for proofreading the manuscript. This work was supported by grants from the NIH (CA102011 and CA130966 to S.-Y. Cheng; EY012509 to A. Kazlauskas; CA87375 to K. Symes), American Cancer Society (RSG CSM-107144), and Pennsylvania Department of Health and Innovative Research Scholar Awards of the Hillman Foundation (to S.-Y. Cheng and B. Hu).

Received for publication May 13, 2010, and accepted in revised form December 22, 2010.

Address correspondence to: Bo Hu, University of Pittsburgh Cancer Institute and Department of Medicine, 5117 Centre Avenue, 2.26, Pittsburgh, Pennsylvania 15213, USA. Phone: 412.623.7791; Fax: 412.623.4840; E-mail: hub@upmc.edu. Or to: Shi-Yuan Cheng, University of Pittsburgh Cancer Institute and Department of Pathology, 5117 Centre Avenue, 2.26f, Pittsburgh, Pennsylvania 15213, USA. Phone: 412.623.3261; Fax: 412.623.4840; E-mail: chengs@upmc.edu.

1. Wen PY, Kesari S. Malignant gliomas in adults. *N Engl J Med.* 2008;359(5):492–507.
2. Furnari FB, et al. Malignant astrocytic glioma: genetics, biology, and paths to treatment. *Genes Dev.* 2007;21(21):2683–2710.
3. TCGA. Comprehensive genomic characterization defines human glioblastoma genes and core pathways. *Nature.* 2008;455(7216):1061–1068.
4. Verhaak RG, et al. Integrated genomic analysis identifies clinically relevant subtypes of glioblastoma characterized by abnormalities in PDGFRA, IDH1, EGFR, and NF1. *Cancer Cell.* 2010;17(1):98–110.
5. Sherr CJ. The INK4a/ARF network in tumour suppression. *Nat Rev Mol Cell Biol.* 2001;2(10):731–737.
6. Serrano M, Lee H, Chin L, Cordon-Cardo C, Beach D, DePinho RA. Role of the INK4a locus in tumor suppression and cell mortality. *Cell.* 1996;85(1):27–37.
7. Bachoo RM, et al. Epidermal growth factor receptor and Ink4a/Arf: convergent mechanisms governing terminal differentiation and transformation along the neural stem cell to astrocyte axis. *Cancer Cell.* 2002;1(3):269–277.
8. Uhrbom L, Dai C, Celestino JC, Rosenblum MK, Fuller GN, Holland EC. Ink4a-Arf loss cooperates with KRas activation in astrocytes and neural progenitors to generate glioblastomas of various morphologies depending on activated Akt. *Cancer Res.* 2002;62(19):5551–5558.
9. Heldin CH, Ostman A, Ronnstrand L. Signal transduction via platelet-derived growth factor receptors. *Biochim Biophys Acta.* 1998;1378(1):F79–F113.
10. Rosenkranz S, DeMali KA, Gelderloos JA, Bazenet C, Kazlauskas A. Identification of the receptor-associated signaling enzymes that are required for platelet-derived growth factor-AA-dependent chemotaxis and DNA synthesis. *J Biol Chem.* 1999; 274(40):28335–28343.
11. Betsholtz C. Insight into the physiological functions of PDGF through genetic studies in mice. *Cytokine Growth Factor Rev.* 2004;15(4):215–228.
12. Van Stry M, Kazlauskas A, Schreiber SL, Symes K. Distinct effectors of platelet-derived growth factor receptor-alpha signaling are required for cell survival during embryogenesis. *Proc Natl Acad Sci U S A.* 2005;102(23):8233–8238.
13. Klinghoffer RA, Hamilton TG, Hoch R, Soriano P. An allelic series at the PDGFalphaR locus indicates unequal contributions of distinct signaling pathways during development. *Dev Cell.* 2002;2(1):103–113.
14. Tallquist M, Kazlauskas A. PDGF signaling in cells and mice. *Cytokine Growth Factor Rev.* 2004;15(4):205–213.
15. Hermanson M, et al. Platelet-derived growth factor and its receptors in human glioma tissue: expression of messenger RNA and protein suggests the presence of autocrine and paracrine loops. *Cancer Res.* 1992;52(11):3213–3219.
16. Dai C, Celestino JC, Okada Y, Louis DN, Fuller GN, Holland EC. PDGF autocrine stimulation dedifferentiates cultured astrocytes and induces oligodendrogliomas and oligoastrocytomas from neural progenitors and astrocytes in vivo. *Genes Dev.* 2001;15(15):1913–1925.
17. Jackson EL, et al. PDGFR alpha-positive B cells are neural stem cells in the adult SVZ that form glioma-like growths in response to increased PDGF signaling. *Neuron.* 2006;51(2):187–199.
18. Stallcup WB, Huang FJ. A role for the NG2 proteoglycan in glioma progression. *Cell Adh Migr.* 2008;2(3):192–201.
19. Ishii N, et al. Frequent co-alterations of TP53, p16/CDKN2A, p14ARF, PTEN tumor suppres-

sor genes in human glioma cell lines. *Brain Pathol.* 1999;9(3):469–479.
20. Wiedemeyer WR, et al. Pattern of retinoblastoma pathway inactivation dictates response to CDK4/6 inhibition in GBM. *Proc Natl Acad Sci U S A.* 2010; 107(25):11501–11506.
21. Fraser M, Bai T, Tsang BK. Akt promotes cisplatin resistance in human ovarian cancer cells through inhibition of p53 phosphorylation and nuclear function. *Int J Cancer.* 2008;122(3):534–546.
22. Wu CJ, O'Rourke DM, Feng GS, Johnson GR, Wang Q, Greene MI. The tyrosine phosphatase SHP-2 is required for mediating phosphatidylinositol 3-kinase/Akt activation by growth factors. *Oncogene.* 2001;20(42):6018–6025.
23. Zhan Y, Counelis GJ, O'Rourke DM. The protein tyrosine phosphatase SHP-2 is required for EGFRvIII oncogenic transformation in human glioblastoma cells. *Exp Cell Res.* 2009;315(14):2343–2357.
24. Wan X, Harkavy B, Shen N, Grohar P, Helman LJ. Rapamycin induces feedback activation of Akt signaling through an IGF-1R-dependent mechanism. *Oncogene.* 2007;26(13):1932–1940.
25. Lu W, Gong D, Bar-Sagi D, Cole PA. Site-specific incorporation of a phosphotyrosine mimetic reveals a role for tyrosine phosphorylation of SHP-2 in cell signaling. *Mol Cell.* 2001;8(4):759–769.
26. Hu X, Holland EC. Applications of mouse glioma models in preclinical trials. *Mutat Res.* 2005; 576(1–2):54–65.
27. Calzolari F, Malatesta P. Recent insights into PDGF-Induced gliomagenesis. *Brain Pathol.* 2010;20(3):527–538.
28. Martinho O, et al. Expression, mutation and copy number analysis of platelet-derived growth factor receptor A (PDGFRA) and its ligand PDGFA in gliomas. *Br J Cancer.* 2009;101(6):973–982.
29. Parsons DW, et al. An integrated genomic analysis of human glioblastoma multiforme. *Science.* 2008;321(5897):1807–1812.
30. Sharpless NE, Ramsey MR, Balasubramanian P, Castrillon DH, DePinho RA. The differential impact of p16(INK4a) or p19(ARF) deficiency on cell growth and tumorigenesis. *Oncogene.* 2004;23(2):379–385.
31. Tchougounova E, Kastemar M, Brasater D, Holland EC, Westermark B, Uhrbom L. Loss of Arf causes tumor progression of PDGFB-induced oligodendroglioma. *Oncogene.* 2007;26(43):6289–6296.
32. Mayo LD, Donner DB. The PTEN, Mdm2, p53 tumor suppressor-oncoprotein network. *Trends Biochem Sci.* 2002;27(9):462–467.
33. Matozaki T, Murata Y, Saito Y, Okazawa H, Ohnishi H. Protein tyrosine phosphatase SHP-2: a proto-oncogene product that promotes Ras activation. *Cancer Sci.* 2009;100(10):1786–1793.
34. Chan G, Kalaitzidis D, Neel BG. The tyrosine phosphatase Shp2 (PTPN11) in cancer. *Cancer Metastasis Rev.* 2008;27(2):179–192.
35. Navis AC, van den Eijnden M, Schepens JT, Hooft van Huijsduijnen R, Wesseling P, Hendriks WJ. Protein tyrosine phosphatases in glioma biology. *Acta Neuropathol.* 2010;119(2):157–175.
36. Cerami E, Demir E, Schultz N, Taylor BS, Sander C. Automated network analysis identifies core pathways in glioblastoma. *PLoS One.* 2010;5(2):e8918.
37. Brennan C, et al. Glioblastoma subclasses can be defined by activity among signal transduction pathways and associated genomic alterations. *PLoS One.* 2009;4(11):e7752.
38. Jarzynka MJ, et al. ELMO1 and Dock180, a bipartite Rac1 guanine nucleotide exchange factor, promote human glioma cell invasion. *Cancer Res.* 2007;67(15):7203–7211.
39. Yiin JJ, et al. Slit2 inhibits glioma cell invasion in the brain by suppression of Cdc42 activity. *Neuro Oncol.* 2009;11(6):779–789.
40. Yoshida S, Shimizu E, Ogura T, Takada M, Sone S. Stimulatory effect of reconstituted basement membrane components (matrigel) on the colony formation of a panel of human lung cancer cell lines in soft agar. *J Cancer Res Clin Oncol.* 1997;123(6):301–309.

Activation of Rac1 by Src-dependent phosphorylation of Dock180^{Y1811} mediates PDGFRα-stimulated glioma tumorigenesis in mice and humans

Haizhong Feng,[1,2] Bo Hu,[1,3] Kun-Wei Liu,[1,2] Yanxin Li,[4] Xinghua Lu,[5] Tao Cheng,[4,6] Jia-Jean Yiin,[7] Songjian Lu,[5] Susan Keezer,[8] Tim Fenton,[9] Frank B. Furnari,[9] Ronald L. Hamilton,[2] Kristiina Vuori,[10] Jann N. Sarkaria,[11] Motoo Nagane,[12] Ryo Nishikawa,[13] Webster K. Cavenee,[9] and Shi-Yuan Cheng[1,2]

[1]Cancer Institute, [2]Department of Pathology, [3]Department of Medicine, [4]Department of Radiation Oncology, and [5]Department of Biomedical Informatics, University of Pittsburgh, Pittsburgh, Pennsylvania, USA. [6]State Key Laboratory of Experimental Hematology, Institute of Hematology and Blood Diseases Hospital, Center for Stem Cell Medicine, Chinese Academy of Medical Sciences and Peking Union Medical College, Tianjin, China. [7]Department of Neurological Surgery, Veteran General Hospital, Taichung, Taiwan. [8]Cell Signaling Technology Inc., Danvers, Massachusetts, USA. [9]Ludwig Institute for Cancer Research and UCSD, School of Medicine, La Jolla, California, USA. [10]Sanford-Burnham Medical Research Institute, La Jolla, California, USA. [11]Department of Radiation Oncology, Mayo Clinic, Rochester, Minnesota, USA. [12]Department of Neurosurgery, Kyorin University Faculty of Medicine, Tokyo, Japan. [13]Department of Neurosurgery, Saitama Medical University, Saitama-ken, Japan.

Two hallmarks of glioblastoma multiforme, the most common malignant brain cancer in humans, are aggressive growth and the ability of single glioma cells to disperse throughout the brain. These characteristics render tumors resistant to current therapies and account for the poor prognosis of patients. Although it is known that oncogenic signaling caused by overexpression of genes such as *PDGFRA* is responsible for robust glioma growth and cell infiltration, the mechanisms underlying glioblastoma malignancy remain largely elusive. Here, we report that PDGFRα signaling in glioblastomas leads to Src-dependent phosphorylation of the guanine nucleotide exchange factor Dock180 at tyrosine 1811 (Dock180^{Y1811}) that results in activation of the GTPase Rac1 and subsequent cell growth and invasion. In human glioma cells, knockdown of Dock180 and reversion with an RNAi-resistant Dock180^{Y1811F} abrogated, whereas an RNAi-resistant Dock180^{WT} rescued, PDGFRα-promoted glioma growth, survival, and invasion. Phosphorylation of Dock180^{Y1811} enhanced its association with CrkII and p130^{Cas}, causing activation of Rac1 and consequent cell motility. Dock180 also associated with PDGFRα to promote cell migration. Finally, phosphorylated Dock180^{Y1811} was detected in clinical samples of gliomas and various types of human cancers, and coexpression of phosphorylated Dock180^{Y1811}, phosphorylated Src^{Y418}, and PDGFRα was predictive of extremely poor prognosis of patients with gliomas. Taken together, our findings provide insight into PDGFRα-stimulated gliomagenesis and suggest that phosphorylated Dock180^{Y1811} contributes to activation of Rac1 in human cancers with *PDGFRA* amplification.

Introduction

Glioblastoma multiforme (GBM), the most common malignant brain cancer in humans, is characterized by high proliferation rates, extensive single-cell infiltration into the adjacent and distant brain parenchyma, and robust neoangiogenesis, which together inevitably confer resistance to current treatment modalities (1–3). Recently, coordinated genomic analyses of large cohorts of clinical GBM specimens rank PDGFRα third among the top 11 amplified genes in GBMs (4, 5). Further integrated analysis revealed that PDGFRα is preferentially amplified within a clinically relevant subtype of glioblastomas (6). Overexpression of PDGFRα and its ligand, PDGF-A, in clinical gliomas is associated with a poor prognosis and shorter survival time for patients (1–3). PDGFRα signaling promotes cell proliferation, survival, and motility through the PI3K, Src, and PLCγ pathways (7). Recently, we reported that activation of PDGFRα signaling drives gliomagenesis of *Ink4a/Arf*-deficient mouse astrocytes and human glioma cells in the brain (8).

Rac1 is a small Rho GTPase and a molecular switch essential for controlling cell movement, survival, and other cellular functions (9). Rac1 is activated by guanine nucleotide exchange factors (GEFs) that promote the exchange of GDP to GTP. There are 2 distinct families of Rho GEFs, those that contain a Dbl-homology (DH) domain and those that are devoid of it. The dedicator of cytokinesis (Dock) family of GEFs, with 11 members in humans, lacks DH domains, but instead has Dock-homology region–1 (DHR-1) and DHR-2 domains (10). Dock1 orthologs in *C. elegans*, *Drosophila*, and mammals (in which it is known as Dock180) modulate cell migration, myoblast fusion, dorsal closure, and cytoskeletal organization through activation of Rac1 (11). Dock180 facilitates GDP/GTP exchange of Rac1 through its DHR-2 domain, but requires formation of a complex with engulfment and cell motility 1 (ELMO1). This bipartite GEF complex synergistically functions upstream of Rac1 and promotes Rac1-dependent cell migration and phagocytosis (11). In cancers, Rac1 mediates tumor cell growth, survival, and invasion in response to various stimuli (9). Although neither Rac1 nor its GEFs, such as Dock180, are known to be overexpressed or mutated in human cancers (10), aberrant and constitutive activation of Rac1 might be involved in tumorigenesis and invasion.

Conflict of interest: The authors have declared that no conflict of interest exists.

Citation for this article: *J Clin Invest.* 2011;121(12):4670–4684. doi:10.1172/JCI58559.

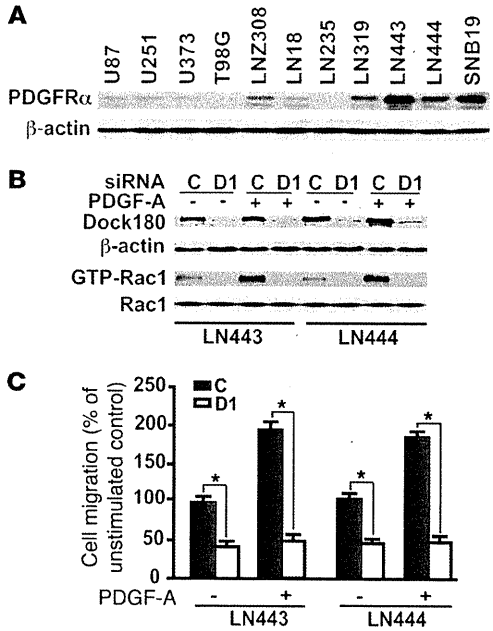

Figure 1
Dock180 mediates PDGFRα-stimulated glioma cell migration in vitro. (**A**) IB assays of endogenous PDGFRα expression in glioma cells. (**B**) LN443 and LN444 glioma cells were transiently transfected with a pool of Dock180 siRNA (D1) or a control siRNA (C). Rac-GTP levels were determined by GTPase activation assays. (**C**) In vitro cell migration assays were performed with a Boyden chamber using cells generated from **B** under serum-starvation conditions. Data are normalized with cell proliferation index (not shown) and presented as percent unstimulated control cells. $^*P < 0.05$. Data (± SD) represent 3 independent experiments with similar results.

Rac1 GEF couples receptor tyrosine kinases (RTKs) to Rac1 (12). PVR, a homolog of PDGF/VEGF receptor in *Drosophila*, is essential for cell migration and spatial guidance of embryonic blood cell precursors (13). Significantly, the Dock180/ELMO1 complex mediates PVR-induced cell migration of these precursor cells through Rac1 during *Drosophila* development (14). Previously, some of us reported that Dock180 plays a critical role in promoting glioma cell invasion through activation of Rac1 (15). Here, in order to determine whether Dock180 activation of Rac1 mediates PDGFRα signaling in glioblastomas, we examined the role of regulatory tyrosine phosphorylation (p-Y) of Dock180 in PDGFRα-promoted glioma tumorigenesis. Our results showed that Dock180 was specifically phosphorylated at tyrosine residue 1811 (p-Dock180^{Y1811}) by PDGFRα-activated Src kinase in gliomas, resulting in stimulation of Dock180 interaction with CrkII and p130^{Cas} as well as subsequent Rac1 activation that culminated in PDGFRα-promoted glioma growth, survival, and invasion. These findings suggest what we believe to be a previously unidentified intervention approach in the treatment of gliomas: targeting the PDGFR/Src/Dock180/Rac1 signaling cascade.

Results

Dock180 mediates PDGFRα-stimulated glioma cell migration and survival in vitro and tumor growth, survival, and invasion in the brain. To establish the role of Dock180 in PDGFRα-stimulated glioma growth, survival, and invasion, we first examined the expression of endogenous PDGFRα in various human glioma cell lines. The LNZ308, LN319, LN443, LN444, and SNB19 glioma cell lines endogenously expressed PDGFRα at moderate to high levels, whereas U87, U251, U373, T98G, LN18, and LN235 glioma cells had lower-level expression of PDGFRα (Figure 1A). To correlate expression levels of PDGFRα proteins with *PDGFRA* gene status in these glioma cells, we performed quantitative PCR analyses (16). Consistent with the levels of PDGFRα protein, increased copy numbers of the *PDGFRA* gene were found in LNZ308, LN319, LN443, LN444, and SNB19 glioma cells. Additionally, in agreement with a previous report (17), *PDGFRA* gene amplification was observed in primary human glioma GBM5 cells, but not in GBM6 cells, GBM14 cells, or other cell lines examined (Supplemental Figure 1; supplemental material available online with this article; doi:10.1172/JCI58559DS1). Heterogeneous levels of PDGFRα expression in various glioma cell lines reflect preferential amplification of *PDGFRA* in the clinically relevant proneural subtype of glioblastomas, but not in other subclasses (6). Moreover, LN443 and LN444 cells also expressed a group of genes that were statistically similar to a subgroup of signature genes in the proneural subtype of clinical GBMs, such as *SOX3*, *GABRA3*, *GALNT13*, *MAPT*, and *NRXN2* (Supplemental Table 1 and ref. 6).

To determine whether Dock180 mediates PDGFRα-stimulated glioma cell growth and migration, we assessed the effect of Dock180 inhibition on PDGFRα stimulation. Knockdown of endogenous Dock180 by a pool of siRNAs markedly impaired basal and PDGF-A–stimulated Rac1 activities and in vitro cell migration of LN443 and LN444 cells (Figure 1, B and C). These data suggest that Dock180 is critical for PDGF-A/PDGFRα–induced Rac1 activation and glioma cell migration.

To determine the function of Dock180 in PDGFRα-stimulated tumorigenesis in vivo, we stably knocked down Dock180 in LN444/PDGF-A gliomas using 2 shRNAs (shRNA1 and shRNA2). Overexpression of PDGF-A by LN444 cells that express endogenous PDGFRα (referred to herein as LN444/PDGF-A cells) promoted the expression of a subgroup of the proneural signature genes (Supplemental Table 1) and gliomagenesis in the brain (8). Knockdown of Dock180 in LN444/PDGF-A cells did not affect expression of exogenous PDGF-A, endogenous PDGFRα, Akt, and Erk1/2 proteins, but reduced the PDGFRα-stimulated phosphorylation of Akt and Erk1/2 compared with the control (Figure 2A). Knockdown of Dock180 by 2 separate shRNAs in LN444/PDGF-A cells had a minimal effect on the population doubling times of cells cultured in media containing 10% FBS, compared with that of LN444/GFP or control shRNA (shControl) cells (Figure 2B). However, knockdown of Dock180 markedly decreased PDGF-A/PDGFRα–stimulated cell survival (Figure 2C; apoptotic index at 48 hours with starvation) and migration (data not shown). These data suggest that depletion of Dock180 inhibits PDGFRα-stimulated Rac1/MAPK and Rac1/Akt signaling as well as glioma cell survival and migration in vitro.

Next, we separately implanted LN444/PDGF-A/shControl, LN444/PDGF-A/Dock180-shRNA1 (referred to herein as shDock180-1), and LN444/PDGF-A/Dock180-shRNA2 (shDock180-2) cells into the brains of mice. Compared with control LN444/GFP gliomas, overexpression of PDGF-A by LN444 gliomas significantly enhanced tumor growth, survival, and invasion (8), whereas knockdown of Dock180 markedly suppressed PDGFRα-stimulated gliomagenesis in the brains of mice (Figure

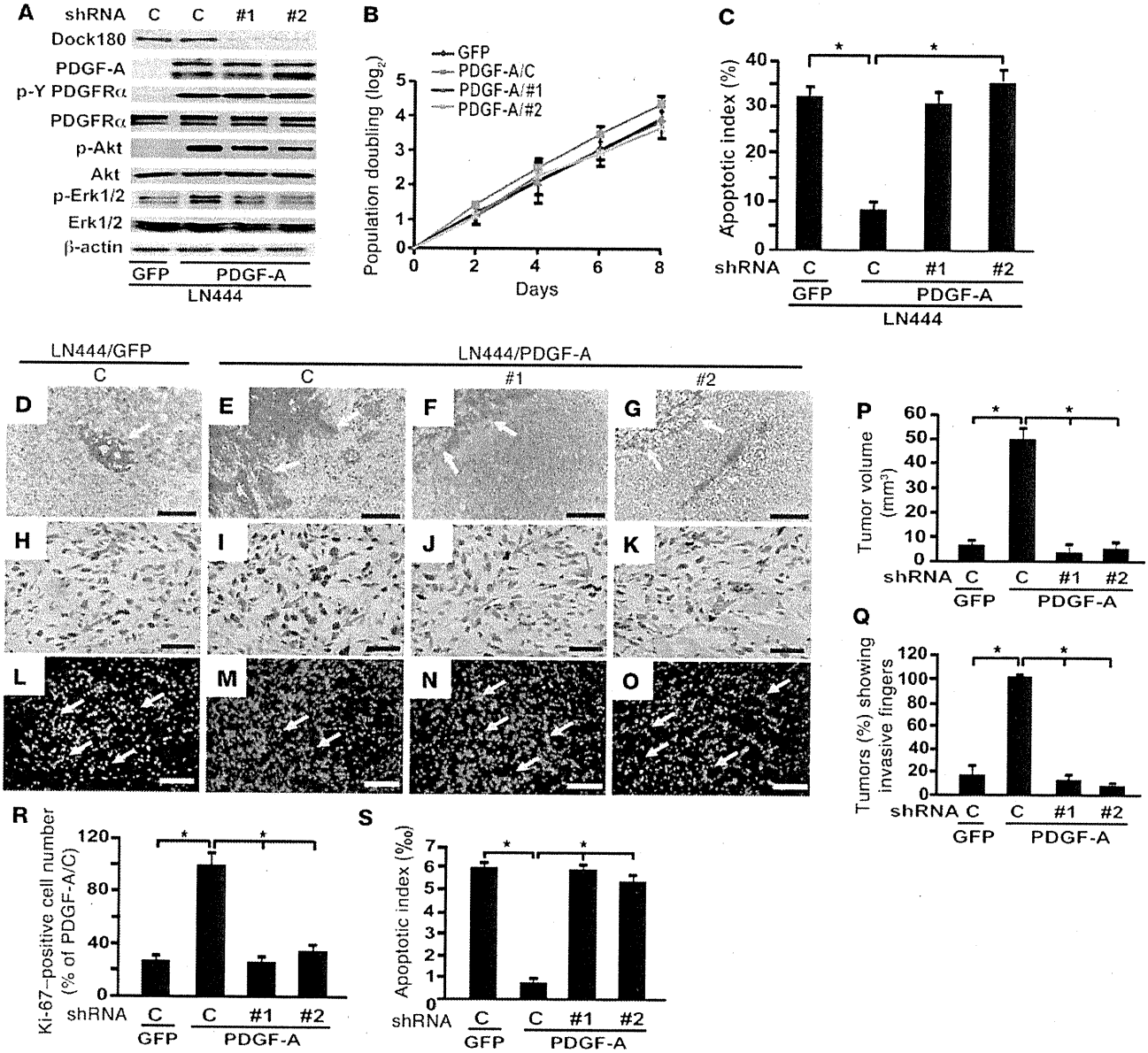

Figure 2

Dock180 mediates PDGFRα-stimulated glioma cell survival in vitro, tumor growth, and invasion in the brain. (**A**) Effect of knockdown of Dock180 with shRNA1 (#1), shRNA2 (#2), or shControl (C) on expression of PDGF-A, p-Y PDGFRα, p-AKT, and p-Erk1/2 in LN444 cells expressing PDGF-A or GFP. (**B**) Cell proliferation assays. (**C**) Cell viability, determined by TUNEL assays after 48-hour serum starvation. (**D–O**) Dock180 depletion inhibited PDGFRα-promoted LN444 glioma growth and invasion in the brain. Shown is representative H&E (**D–G**), Ki-67 (**H–K**), and TUNEL (**L–O**) staining of brain sections from 5 mice per group. Arrows denote invasive tumor cells (**E**), noninvasive tumor borders (**D**, **F**, and **G**), and positively stained tumor cells (**H–O**). Scale bars: 200 μm (**D–G**); 50 μm (**H–K**); 100 μm (**L–O**). (**P–S**) Quantification of tumor size (**P**), percent of tumors showing invasive fingers (**Q**), Ki-67 staining (**R**), and TUNEL staining (**S**). Data (± SD) represent 3 independent experiments with similar results. *$P < 0.05$.

2, D–S, and Supplemental Figure 2). When various brain sections from the different tumors were examined by immunohistochemical (IHC) staining, ectopically expressed PDGF-A enhanced cell proliferation compared with the control (Figure 2, H, I, and R, and Supplemental Figure 2, I and J). However, depletion of Dock180 significantly decreased LN444 tumor cell proliferation compared with shControl tumors (Figure 2, I–K and R, and Supplemental Figure 2, J–L). To a similar extent, compared with LN444/GFP, overexpression of PDGF-A resulted in a marked decrease in cell apoptosis (Figure 2, L, M, and S, and Supplemental Figure 2, N and M). Knockdown of Dock180 in LN444/PDGF-A tumors also significantly increased cell apoptosis compared with shControl tumors (Figure 2, M–O and S, and Supplemental Figure 2, N–P). Taken together, these results suggest that specific activation of

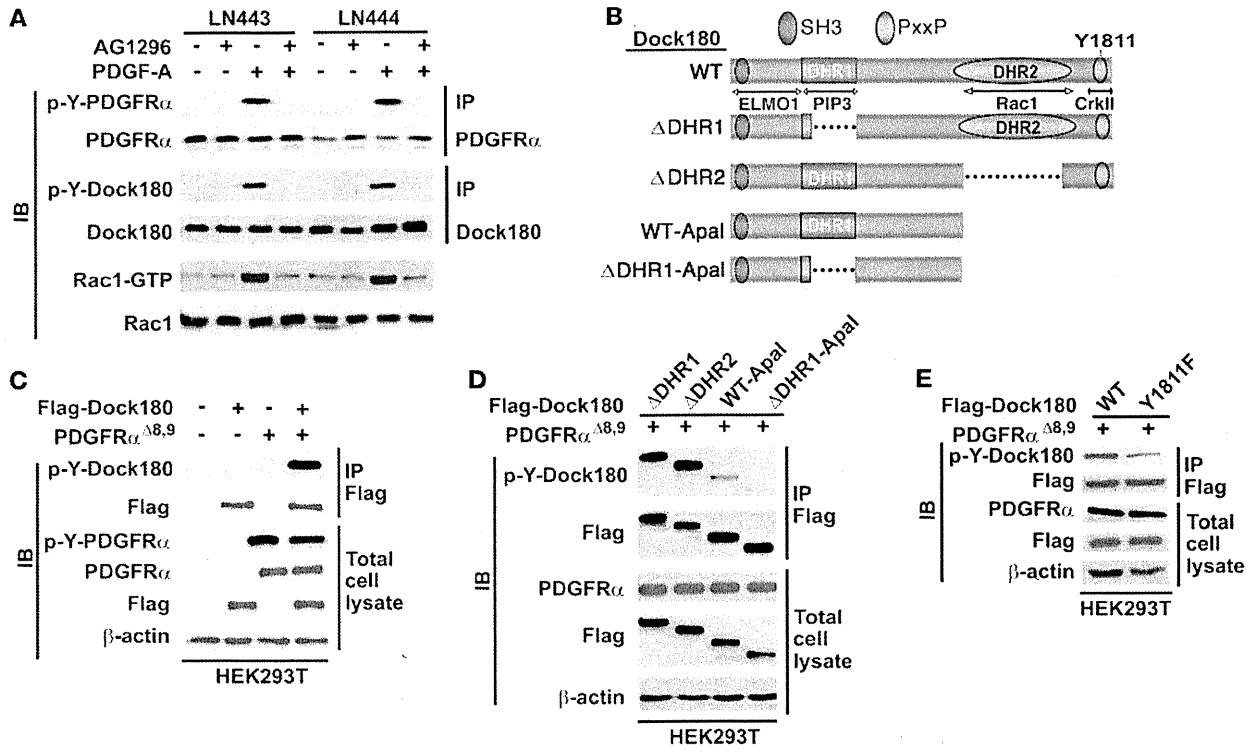

F

Human	1801	PLPLKGSVADYGNLMENQD	1819
Monkey	775	PLPLKGSVADYGNLMENQD	793
Mouse	1801	PLPLKGNMADYGNLMENQD	1819
Rat	1801	PLPLKGNMADYGNLMENQD	1819
Chicken	1801	PLPLKGSMADYGNLMESQD	1819
Horse	1794	PLPLKGSTADYGNLMENQD	1812
Dog	1794	PLPLKGSMADYGNLMENQD	1812
Cattle	1831	PLPLKGTSTDYGTLNENLD	1849
Zebrafish	1802	PLPVKSSMGDYGNLMDNSD	1820
Opossum	1029	PLPLKGSTADYGNLMENPD	1047

Figure 3

PDGF-A stimulation of PDGFRα induces p-Y of Dock180^{Y1811}. (**A**) PDGF-A induced p-Y of Dock180 and activated Rac1 in serum-starved LN443 and LN444 cells pretreated with or without the PDGFRα inhibitor AG1296 (20 μM) for 1 hour followed by PDGF-A (50 ng/ml) treatment for 5 minutes. (**B**) Schematics of Dock180^{WT} and various Dock180 deletion mutants. (**C** and **D**) A CA PDGFRα (PDGFRα^{Δ8,9}) induced p-Y of Dock180 at the Y1811 residue. Dock180^{WT} or the indicated Dock180 mutants and PDGFRα^{Δ8,9} were cotransfected into HEK293T cells. (**E**) Y1811 was a major PDGFRα-induced p-Y site. Experiments were similar to **C**, except Dock180^{WT} or Dock180^{Y1811F} was used. (**F**) Y1811 is conserved in Dock180 from various species. (**A** and **C**–**E**) p-Y of Dock180 was detected with a pan-phosphotyrosine antibody (4G10). Data represent 2 independent experiments with similar results.

PDGFRα by PDGF-A enhances glioma growth, survival, and invasion and that Dock180 is required for PDGFRα-promoted gliomagenesis in the brain.

Dock180 is specifically phosphorylated at Y1811 by PDGFRα stimulation in glioma cells. Since Dock180 activates Rac1 (11) and mediates PVR-induced cell migration in vivo (14), we hypothesized that PDGFRα signaling promotes glioma cell growth, survival, and invasion through p-Y of Dock180, leading to activation of Rac1. To test this hypothesis, we first examined whether PDGF-A stimulation induces p-Y of endogenous Dock180 in glioma cells. PDGF-A stimulation of LN443 or LN444 glioma cells induced distinct p-Y of PDGFRα, p-Y of Dock180, and activation of Rac1, whereas inhibition of PDGF-A stimulation by a PDGFR inhibitor, AG1296 (which selectively inhibits RTK activities of PDGFRα and PDGFRβ and PDGF-mediated signaling in cells; ref. 18), impaired PDGF-A–induced p-Y of PDGFRα, p-Y of Dock180, and Rac1 activation in glioma cells (Figure 3A).

Next, we computationally examined potential p-Y sites of the Dock180 protein (using the SCANSITE tool, http://scansite.mit.edu; and the NetPhosK 1.0 server, http://www.cbs.dtu.dk/services/NetPhosK) and identified 27 hypothetical p-Y sites, including Y1811, a residue in Dock180 predicted to be a target of Src and other kinases. To determine whether PDGFRα stimulates glioma growth, survival, and invasion and Rac1 activation through one or more specific p-Y sites of Dock180, we constructed various Dock180 deletion mutants (Figure 3B) and cotransfected these DNAs, together with a glioma-derived and constitutively active (CA)

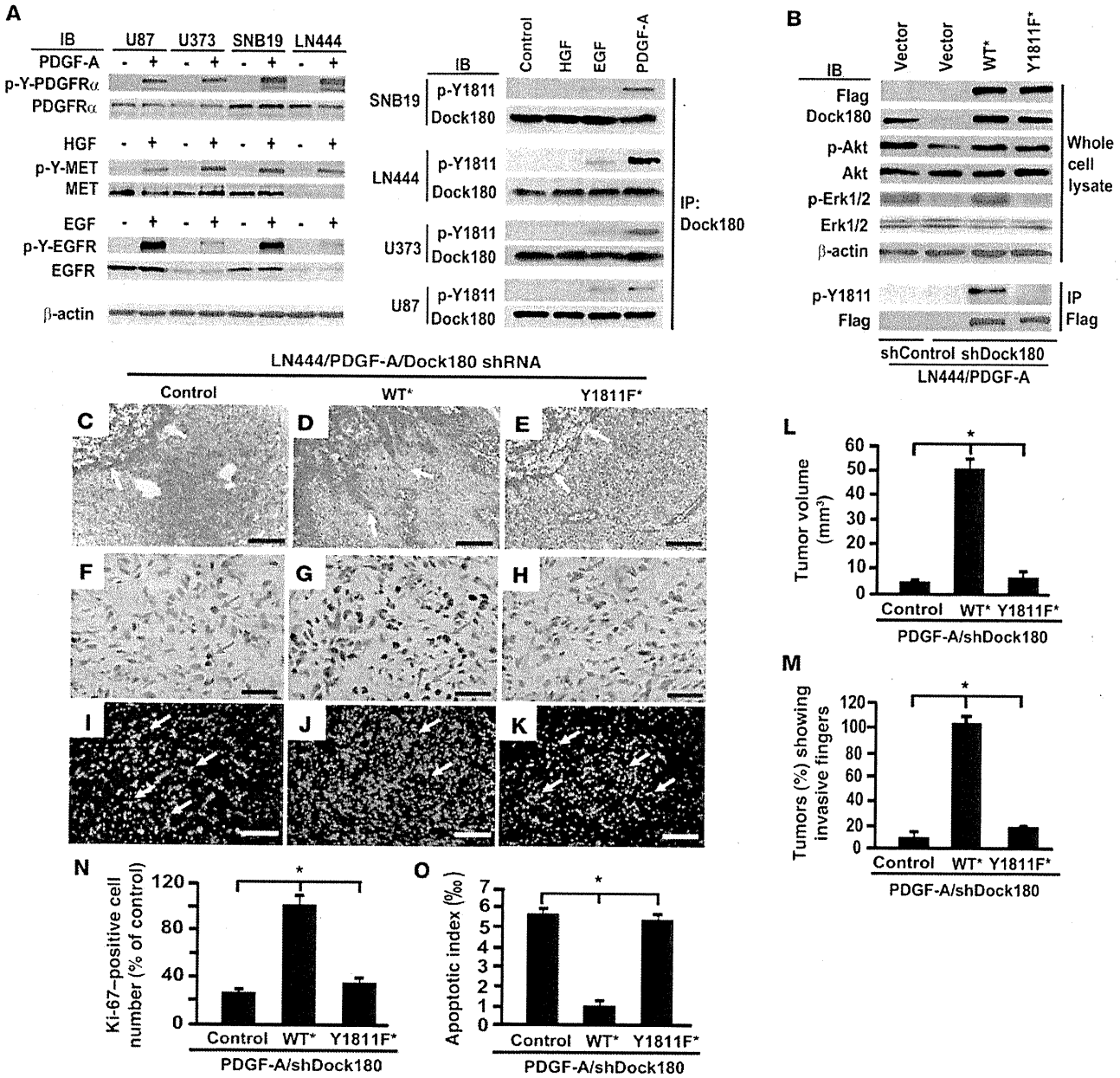

Figure 4

p-Y of Dock180^{Y1811} is required for PDGFRα-promoted glioma growth and invasion in the brain. (**A**) U87, U373, SNB19, and LN444 cells were serum-starved for 24 hours and treated with or without 50 ng/ml PDGF-A, 50 ng/ml EGF, or 40 ng/ml HGF for 5 minutes. Anti–c-Met (p-Y1230/Y1234/Y1235), anti–p-PDGFRα (p-Y754), and anti–p-EGFR (p-Y1045) antibodies were used to examine p-Y of c-Met, PDGFRα, and EGFR, respectively. (**B**) Effect of reexpression of shRNA-resistant Flag-tagged Dock180^{WT*}, Dock180^{Y1811F*}, or vector control on p-Akt and p-Erk1/2 in LN444/PDGF-A/shRNA cells. (**A** and **B**) A specific anti-phosphotyrosine Dock180^{Y1811} antibody was used to detect p-Y of endogenous Dock180 in these cells. (**C**–**K**) Reexpression of shRNA-resistant Dock180^{WT*}, but not Dock180^{Y1811F*}, restored PDGFRα-promoted tumorigenesis of LN444/PDGF-A/shRNA gliomas in the brain. Shown is representative H&E (**C**–**E**), Ki-67 (**F**–**H**), and TUNEL (**I**–**K**) staining of 5 mice per group. Arrows indicate invasive tumor cells (**D**), noninvasive tumor borders (**C** and **E**), or positively stained tumor cells (**F**–**K**). Scale bars: 200 μm (**C**–**E**); 50 μm (**F**–**H**); 100 μm (**I**–**K**). (**L**–**O**) Quantifications of tumor size (**L**), percent of tumors showing invasive fingers (**M**), Ki-67 staining (**N**), and TUNEL staining (**O**). Data (± SD) represent 3 independent experiments with similar results. *$P < 0.05$.

PDGFRα^{Δ8,9} mutant (19), into human HEK293T cells. Coexpression of PDGFRα^{Δ8,9} with Dock180^{WT} induced p-Y of Dock180. Deletions of the DHR-1 (ΔDHR1) or DHR-2 (ΔDHR2) domain from the Dock180 peptide that interacts with PIP_3 or Rac1, respectively (11), had no effect on PDGFRα^{Δ8,9}-induced p-Y of Dock180 (Figure 3, C and D). However, removal of a C-terminal segment, including the DHR2 domain (WT-ApaI), markedly reduced PDGFRα^{Δ8,9}-induced p-Y, whereas an N-terminal segment lacking the DHR-1 domain

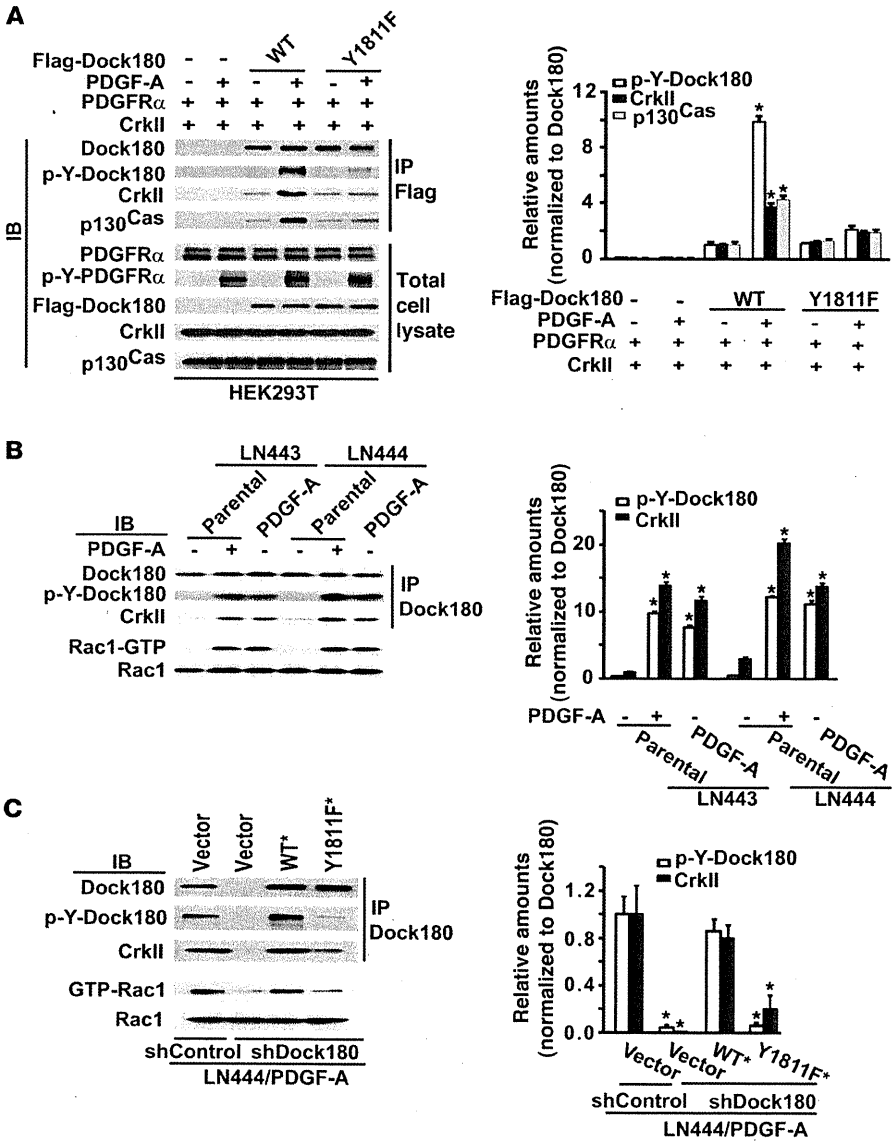

Figure 5

p-Y of Dock180^{Y1811} regulates PDGFRα-stimulated recruitment of CrkII and p130^{Cas} and activity of Rac1. (**A**) PDGF-A induced p-Y of PDGFRα and Dock180, but not Dock180^{Y1811F}, and protein association of Dock180^{WT}, but not Dock180^{Y1811F}, with CrkII and p130^{Cas}. (**B**) PDGF-A induced the formation of a Dock180/CrkII/p130^{Cas} complex and activated Rac1 in LN443 and LN444 cells stimulated by PDGF-A. (**C**) Reexpression of shRNA-resistant Flag-tagged Dock180^{WT*}, but not Dock180^{Y1811F*}, restored the PDGF-A–induced formation of a Dock180/CrkII/p130^{Cas} complex and activation of Rac1 in LN444/PDGF-A/shDock180 glioma cells. (**A**–**C**) p-Y of Dock180 was detected with a pan-phosphotyrosine antibody (4G10). Relative p-Y of Dock180, CrkII, or p130^{Cas} was determined by Image J and normalized to the amount of Dock180 in IP. $^{*}P < 0.05$. Data (± SD) represent 3 independent experiments with similar results.

(ΔDHR1-ApaI) further diminished the induced p-Y of Dock180, suggestive of a major p-Y site located at the C terminus. Examination of potential p-Y sites within the targeted domain of Dock180 identified a single p-Y candidate site at Y1811 (Figure 3B). To ascertain that Y1811 is a major p-Y site of Dock180 induced by PDGFRα, Y1811 was mutated to phenylalanine (F) in the full-length Dock180 protein. PDGFRα^{Δ8,9}-induced p-Y was markedly reduced for Dock180^{Y1811F} compared with the stimulated p-Y of Dock180^{WT} (Figure 3E). Incomplete abrogation of PDGF-A–induced p-Y of Dock180 corroborates with the results in Figure 3D, which indicates that there is a minor p-Y site in the DHR-1 domain of Dock180 protein. When we examined aa sequences surrounding Y1811 in Dock180 of various species and Dock family members, we found that Y1811 and most of its surrounding aa residues were highly conserved in Dock180 among these species (Figure 3F), but not other members of the Dock family (Supplemental Figure 3). Taken together, these results suggest Y1811 of Dock180 as a major p-Y site that is specifically phosphorylated by PDGFRα in glioma cells.

p-Dock180^{Y1811} is required for PDGFRα-stimulated glioma cell migration and survival in vitro and tumor growth, survival, and invasion in the brain. We generated a rabbit polyclonal antibody that specifically recognizes the p-Dock180^{Y1811} protein. This anti–p-Dock180^{Y1811} antibody detected a strong signal of p-Y of endogenous Dock180 in U87, U373, SNB19, and LN444 glioma cells stimulated with PDGF-A, but weak or absent signal in these glioma cells treated with EGF or HGF, compared with the control (Figure 4A), indicative of its selectivity for PDGFRα-induced p-Dock180^{Y1811}. Next, we stably reexpressed an shRNA-resistant Dock180^{WT*} or Dock180^{Y1811F*} in poorly tumorigenic LN444/PDGF-A/shDock180-2 cells in which endogenous Dock180 had been stably depleted (Figure 2A). The exogenous Dock180^{WT*} or Dock180^{Y1811F*} proteins were expressed at levels comparable to those of endogenous Dock180 in shControl-expressing cells (Figure 4B). The anti–p-Dock180^{Y1811} antibody detected p-Y of Dock180^{WT*}, but not Dock180^{Y1811F*}, proteins in these cells. Moreover, Dock180^{WT*}, but not Dock180^{Y1811F*}, rescued the PDGF-A–induced phosphorylation of Erk1/2. However, both Dock180^{WT*} and Dock180^{Y1811F*}

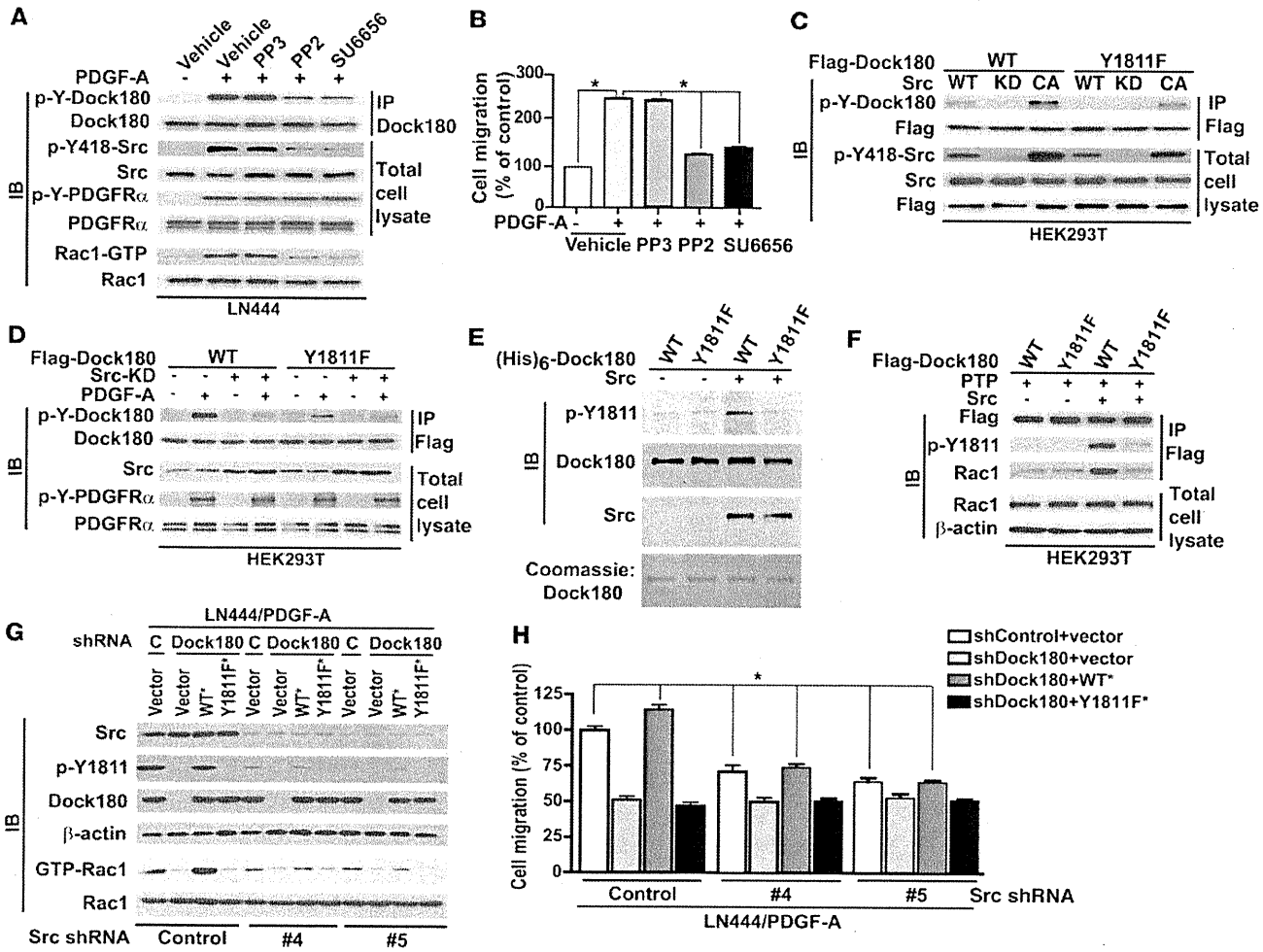

Figure 6

Src mediates PDGFRα stimulation of p-Y of Dock180^{Y1811}, activation of Rac1, and glioma cell migration. (**A**) Serum-starved LN444 cells were pretreated with or without PP3 (2 μM), PP2 (2 μM), and SU6656 (2 μM) for 2 hours, and then stimulated with or without PDGF-A (50 ng/ml) for 5 minutes. (**B**) In vitro cell migration assays were performed and analyzed as in Figure 1C. (**C**) Src phosphorylates Dock180. Dock180^{WT} or Dock180^{Y1811F} and WT, KD, or CA Src were separately cotransfected into HEK293T cells. (**D**) Dock180^{WT} or Dock180^{Y1811F} and KD Src were separately cotransfected into HEK293T cells that were serum-starved and treated with or without PDGF-A. (**E**) In vitro Src kinase assay using recombinant active Src and (His)$_6$-Dock180^{WT} or (His)$_6$-Dock180^{Y1811F} proteins. Purified (His)$_6$-Dock180^{WT} or (His)$_6$-Dock180^{Y1811F} proteins were visualized by Coomassie brilliant blue staining. (**F**) Src phosphorylation of Dock180^{Y1811} enhanced the association of Dock180 to Rac1. PTP, a recombinant YOP PTP. (**G**) Knockdown of Src inhibited PDGF-A–induced p-Y of Dock180^{Y1811} and Rac1 activation. LN444/PDGF-A/shDock180 or LN444/PDGF-A/shControl cells with or without restored Dock180^{WT*}, Dock180^{Y1811F*}, or pLVX-Puro vector control were transfected with Src shRNA4 (#4), Src shRNA5 (#5), or a shGFP control. (**H**) In vitro cell migration assays were performed and analyzed as in Figure 1C. (**A**, **C**, and **D**) p-Y of Dock180 was detected with a pan-phosphotyrosine antibody (4G10). (**E**–**G**) p-Y1811 was detected with a specific anti–p-Dock180^{Y1811} antibody. Data (± SD) represent 3 independent experiments with similar results. *$P < 0.05$.

rescued the PDGF-A–induced phosphorylation of Akt (Figure 4B), which suggests that p-Dock180^{Y1811} is important for Rac1/MAPK signaling. Although no appreciable effect was seen on cell population doubling (Supplemental Figure 4A), reexpression of Dock180^{WT*}, but not Dock180^{Y1811F*}, in LN444/PDGF-A/shDock180-2 cells restored PDGF-A–stimulated cell viability and migration in vitro (Supplemental Figure 4, B and C). Importantly, when various engineered LN444 cells were implanted into the brains of mice, restoration of Dock180^{WT*}, but not Dock180^{Y1811F*}, in poorly tumorigenic LN444/PDGF-A/shDock180-2 cells rescued PDGFRα-promoted tumor growth, survival, and invasion (Figure 4, C–E, L, and M, and Supplemental Figure 5, A–F). Additionally, reexpression of Dock180^{WT*}, but not Dock180^{Y1811F*}, in LN444/PDGF-A/shDock180-2 gliomas also rescued PDGFRα-induced cell proliferation and inhibited cell apoptosis (Figure 4, F–K, N, and O, and Supplemental Figure 5, G–L). In addition, compared with the control or Dock180^{Y1811F*}, reexpression of Dock180^{WT*} by LN444/PDGF-A/shDock180-2 gliomas also significantly increased tumor angiogenesis and microglia growth, but had a minimal effect on the tumor infiltration of macrophages (Supplemental Figure 6). Taken together, these data suggest that p-Y of Dock180^{Y1811} is necessary for PDGFRα-stimulated glioma growth, survival, and invasion in the brain.

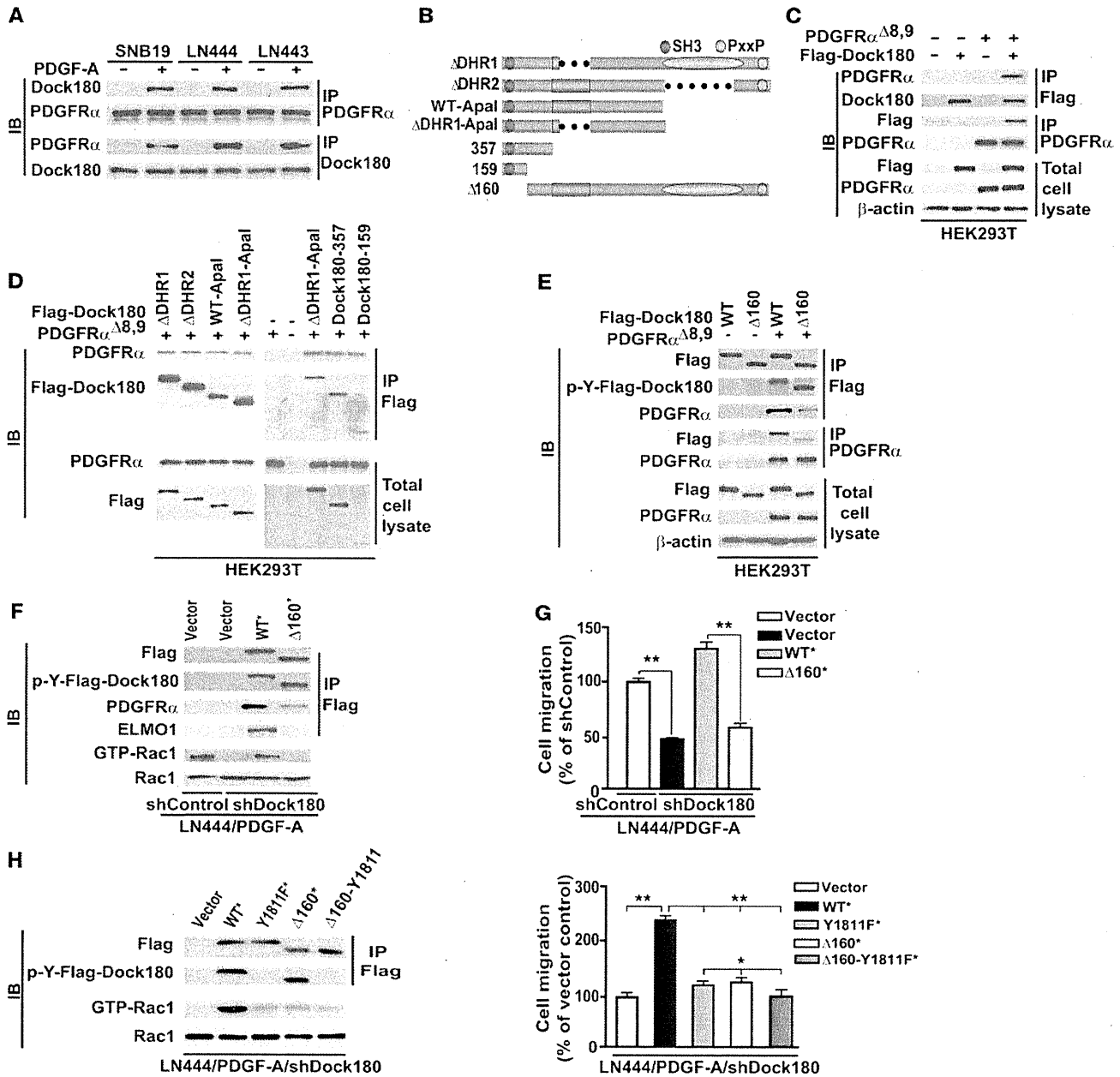

Figure 7

PDGF-A–induced association of Dock180 with PDGFRα is required for PDGFRα-promoted glioma cell migration. (**A**) PDGF-A induced association of Dock180 with PDGFRα in glioma cells. (**B**) Schematics of Dock180^{WT} and various Dock180 deletion mutants. (**C–E**) Dock180^{WT} or indicated Dock180 mutants was separately cotransfected with or without PDGFRα$^{\Delta 8,9}$ into HEK293T cells. (**C** and **D**) Dock180 interacted with PDGFRα through its N-terminal region with aa residues 1–159. (**E**) Removal of 1–159 aa of Dock180 (Dock180$^{\Delta 160}$) inhibited the induced interaction of Dock180 with PDGFRα without affecting p-Y Dock180 in HEK293T cells. (**F**) Dock180$^{\Delta 160}$ inhibited interaction of Dock180 with PDGFRα, ELMO1, and Rac1 activation without affecting p-Y of Dock180 in LN444/PDGF-A cells. (**G**) In vitro cell migration assays were performed and analyzed as in Figure 1C. (**H**) The double mutation Dock180$^{\Delta 160\text{-}Y1811F}$ had an additive effect on inhibition of PDGFRα-induced Rac1 activation and cell migration compared with that caused by single Dock180^{Y1811F} or Dock180$^{\Delta 160}$ mutation. (**A**, **C–F**, and **H**) Co-IP experiments were performed using anti-PDGFRα, anti-Dock180, anti-Flag, or anti-phosphotyrosine (4G10) antibodies. Data (± SD) represent 3 independent experiments with similar results. *$P < 0.05$; **$P < 0.001$.

p-Dock180^{Y1811} mediates PDGFRα-stimulated recruitment of CrkII and p130^{Cas} and Rac1 activation. Y1811 is located at the C-terminal domain of Dock180, which interacts with CrkII and mediates Dock180/CrkII/p130^{Cas}/Rac1 signaling in promoting cell motility (Figure 3B and ref. 11). Thus, we sought to determine whether p-Dock180^{Y1811} is critical for PDGFRα-induced formation of a Dock180/CrkII/p130^{Cas} complex and activation of Rac1 in glioma cells. WT PDGFRα and CrkII were coexpressed with

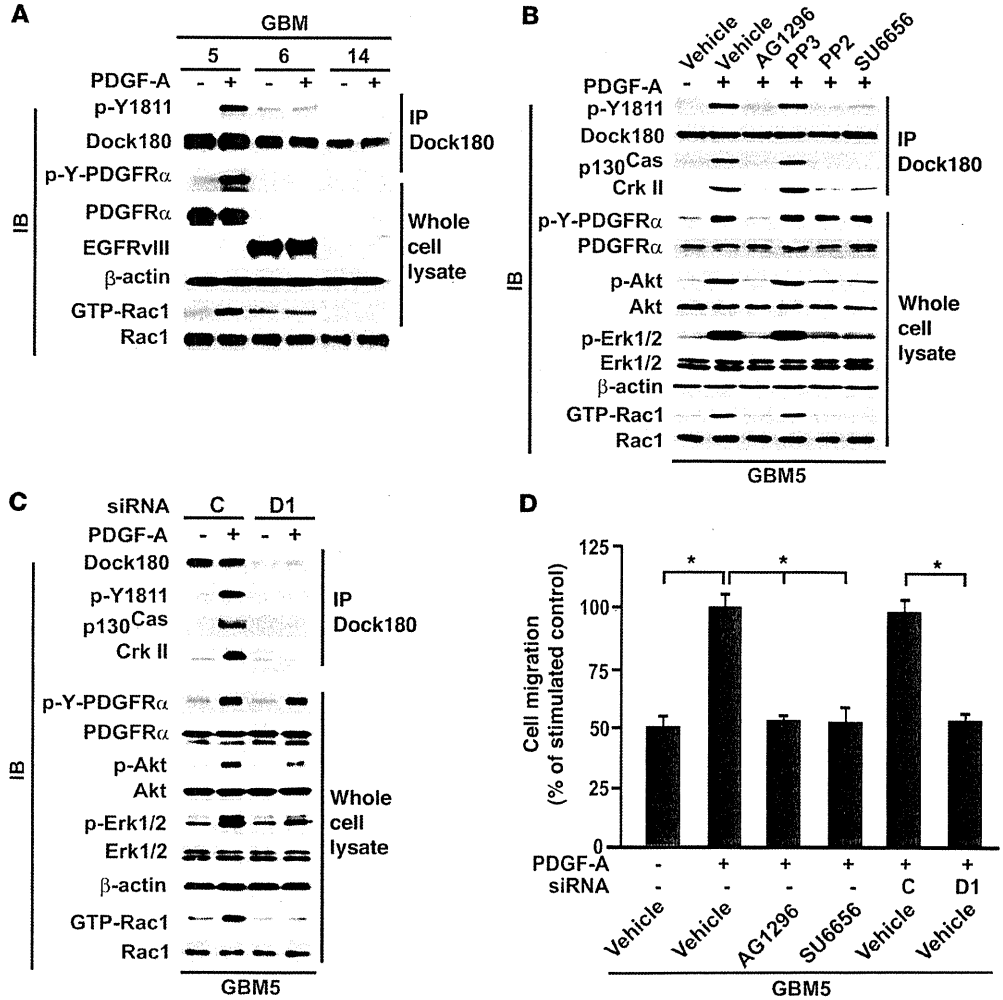

Figure 8

Inhibition of p-Dock180^{Y1811} by inhibitors of PDGFRα or Src, or by Dock180 siRNA, impairs PDGFRα-stimulated Dock180 association with p130^{Cas}, CrkII, p-Akt, p-Erk1/2, and Rac1 activities as well as cell migration in GBM5 cells with PDGFRα overexpression. (**A**) PDGF-A stimulation promoted p-Y of Dock180^{Y1811} in GBM5 cells. (**B**) PDGFRα or Src inhibitors blocked PDGFRα-stimulated p-Y of Dock180^{Y1811} as well as Dock180 association with p130^{Cas}, CrkII, p-Akt, p-Erk1/2, and Rac1 activities in GBM5 cells. (**C**) Knockdown of Dock180 by siRNA inhibited PDGFRα-stimulated p-Y of Dock180Y^{1811} and Dock180 association with p130^{Cas}, CrkII, p-Akt, p-Erk1/2 and Rac1 activities in GBM5 cells. C, control siRNA; D1, Dock180 siRNA pool. (**D**) Treatment with PDGFRα or Src inhibitors or Dock180 siRNA inhibited PDGFRα-stimulated cell migration in GBM5 cells. (**A–C**) An anti–p-Dock180^{Y1811} antibody was used to detect p-Dock180^{Y1811} (p-Y1811). Data (± SD) represent 3 independent experiments with similar results. *$P < 0.05$.

either Flag-tagged Dock180^{WT} or Flag-tagged Dock180^{Y1811F} in HEK293T cells. PDGF-A stimulation induced p-Y of WT PDGFRα and Dock180^{WT} and association of Dock180^{WT} with CrkII and p130^{Cas} (Figure 5A). In contrast, co-IP experiments showed that the Dock180^{Y1811F} mutation substantially attenuated PDGFRα-induced p-Y of Dock180 and interaction of Dock180 with CrkII and p130^{Cas}, whereas no effect on p-Y of PDGFRα was observed. Treatment of LN443 or LN444 cells with exogenous PDGF-A or ectopic PDGF-A expression induced the association of Dock180 with CrkII and p130^{Cas} and activated Rac1 (Figure 5B). However, restoration of Dock180^{Y1811F*}, but not Dock180^{WT*}, in LN444/PDGF-A/shDock180 cells in which endogenous Dock180 had been depleted impeded PDGF-A induction of p-Dock180^{Y1811}, association of Dock180 with CrkII, and activation of Rac1 (Figure 5C). These results indicate that p-Dock180^{Y1811} mediates PDGFRα-induced association of Dock180 with CrkII and p130^{Cas} and activation of Rac1 in glioma cells.

Src mediates PDGFRα stimulation of p-Dock180^{Y1811} and glioma cell migration. In addition to the potential p-Y sites of Dock180, our computational analysis also suggested Dock180^{Y1811} as a putative substrate site for Src. Src is a non-RTK that plays a crucial role in tumor progression and tumorigenesis promoted by aberrant activation of RTK signaling, including PDGFR (20). Thus, we hypothesized that PDGFRα promotes glioma tumorigenesis and invasion through Src stimulation of p-Dock180^{Y1811} and activation of Rac1. To test this hypothesis, LN444 cells were pretreated with or without the Src inhibitor PP2, its PP3 inactive stereoisomer, or SU6656, a structurally unrelated Src inhibitor,

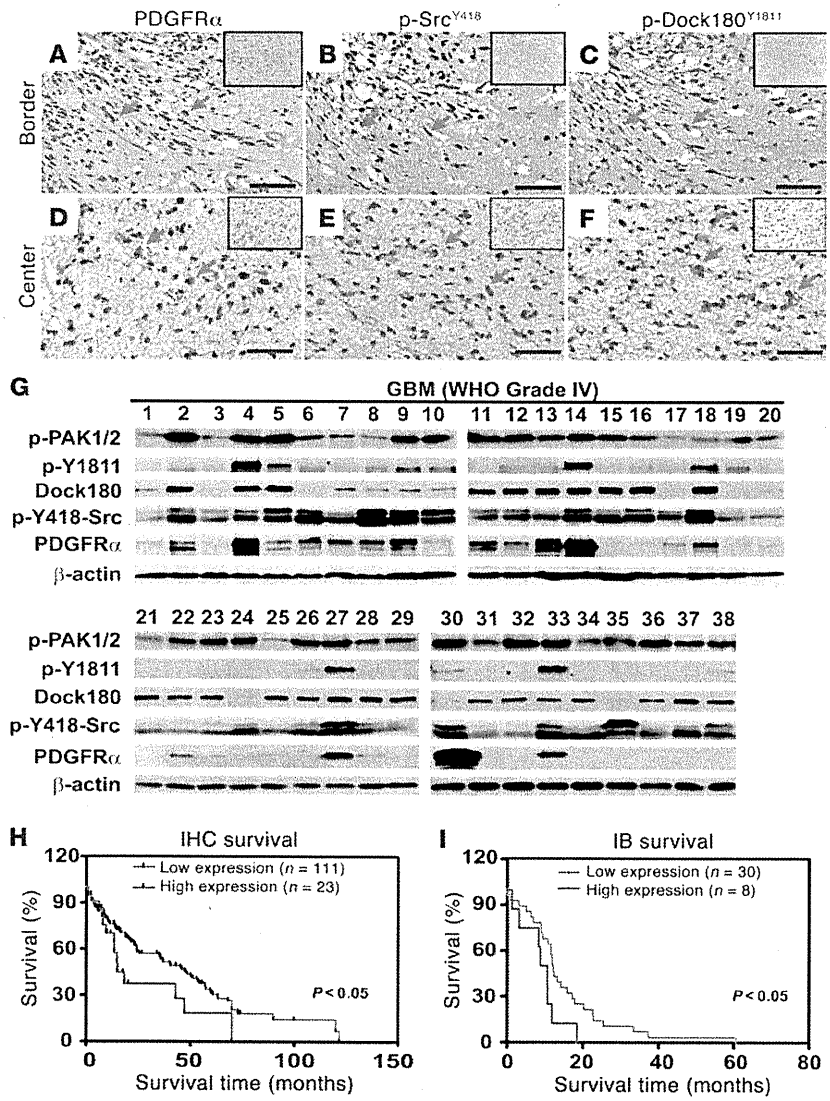

Figure 9
p-Dock180^{Y1811}, p-Src^{Y418}, and PDGFRα are coexpressed in primary human glioma specimens. (**A–F**) In total, 134 clinical primary glioma specimens, including WHO grades II–IV, were analyzed by IHC staining for PDGFRα, p-Src^{Y418}, and p-Dock180^{Y1811}. Specimens expressing PDGFRα and/or p-Dock180^{Y1811} are listed in Supplemental Table 2. Representative images of serial sections of a WHO grade IV GBM tissue using anti-PDGFRα (**A** and **D**), anti–p-Src^{Y418} (**B** and **E**), and anti-p-Dock180^{Y1811} (**C** and **F**) antibodies are shown. (**A–C**) Invasive border area. (**D–F**) Central region. Insets show isotype-matched IgG controls of the identical area (original magnification, ×400). Arrows denote positive staining. Scale bars: 50 μm. (**G**) Expression of PDGFRα, p-Src^{Y418}, p-Dock180^{Y1811} (using the specific anti–p-Dock180^{Y1811} antibody), and p-PAK1/2 (p-PAK1^{T423}/PAK2^{T402}) in a separate and independent cohort of a total of 38 snap-frozen GBM specimens. Dock180 and β-actin were used as loading controls. (**H** and **I**) Kaplan-Meier analyses of patients with high PDGFRα/p-Dock180^{Y1811}–expressing tumors versus low PDGFRα/p-Dock180^{Y1811}–expressing tumors in IHC staining (**H**) and IB (**I**) assays of WHO grade II–IV gliomas. *P* values were calculated by log-rank test. Black bars, censored data. Data represent 2 independent experiments with similar results.

prior to stimulation with PDGF-A. Treatment of LN444 cells with PP2 or SU6656, but not vehicle control or PP3, markedly decreased PDGF-A–induced p-Y of Dock180, p-Src^{Y418}, and Rac1 activity (Figure 6A). Of note, the PDGF-A–induced p-Y of PDGFRα remained unchanged in the presence or absence of the Src inhibitors. When various treated LN444 cells were analyzed for in vitro migration, inhibition of Src by PP2 or SU6656, but not the control or PP3, significantly abrogated PDGF-A–induced cell migration (Figure 6B). The incomplete inhibition of PDGF-A–induced p-Y of Dock180 by Src inhibitors could be due to a minor p-Y site in Dock180 (Figure 3), which suggests that other kinases, such as PI3K, may contribute to p-Y of Dock180. To test this possibility, we treated LN444 cells with the PI3K inhibitor LY294002 prior to PDGF-A stimulation. We found that inhibition of PI3K did not affect PDGF-A–induced p-Y of Dock180, but markedly decreased PDGF-A–induced Rac1 activity and cell migration, compared with controls (Supplemental Figure 7 and ref. 21), which suggests that a different kinase mediates PDGF-A–induced p-Y at this minor site.

To determine whether Src phosphorylates Dock180^{Y1811}, we separately cotransfected cDNAs of Flag-tagged Dock180^{WT} or Flag-tagged Dock180^{Y1811F} together with Src WT, a kinase-dead (KD) mutant, or a CA mutant (Y527F) into HEK293T cells. Without stimulation, CA Src, but not WT or KD Src, induced p-Y of Flag-tagged Dock180^{WT} (Figure 6C). In contrast, coexpression of Flag-tagged Dock180^{Y1811F} with CA Src severely reduced its p-Y, whereas no p-Dock180^{Y1811F} was detected when WT or KD Src were coexpressed in HEK293T cells. To validate that Src mediates PDGFRα stimulation of p-Dock180^{Y1811}, Flag-tagged Dock180^{WT} and Flag-tagged Dock180^{Y1811F} were separately cotransfected with WT PDGFRα and KD Src mutant into HEK293T cells. After 48 hours, cells were serum starved and stimulated with PDGF-A. Treatment with PDGF-A induced p-Y of PDGFRα and Dock180, whereas coexpression of KD Src markedly inhibited PDGF-A–induced p-Y of Dock180, with no effect on PDGF-A–induced p-Y of PDGFRα (Figure 6D). Furthermore, Dock180p^{Y1811F} significantly prevented PDGF-A–stimulated p-Y of Dock180, but not p-Y of PDGFRα. Coexpression of KD Src with Dock180^{Y1811F} further diminished

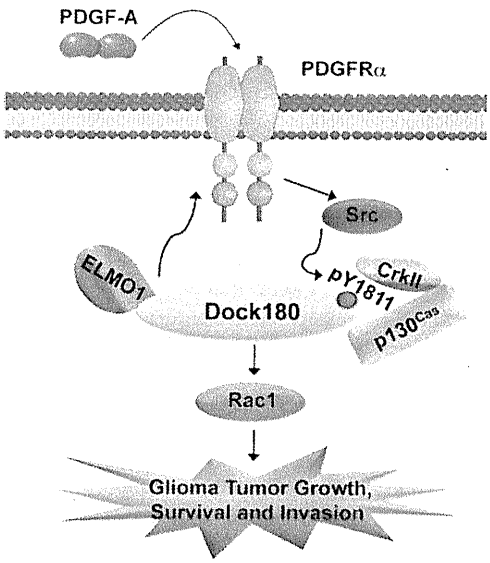

Figure 10
Working model of PDGFRα/Src/Dock180/CrkII/p130^{Cas}/Rac1 signaling in glioma tumor growth, survival, and invasion. PDGF-A activation of PDGFRα induces Src-dependent p-Y of Dock180^{Y1811} at the C terminus, promoting its association with CrkII and p130^{Cas} as well as Rac1 activities and leading to increased glioma tumor growth, survival, and invasion. PDGF-A activation of PDGFRα also induces an association of the receptor with the N terminus of Dock180, resulting in enhanced Rac1 activities and glioma migration.

PDGF-A–stimulated p-Y of Dock180 (Figure 6D). Again, similar to our data in Figure 3, the residual PDGF-A–induced p-Y of Dock180 (Figure 6, C and D) was attributable to the existence of a minor p-Y site in Dock180 that is a substrate for another kinase.

Next, we performed an in vitro p-Y assay by incubating purified recombinant (His)$_6$-Dock180^{WT} or (His)$_6$-Dock180^{Y1811F} proteins with a recombinant active Src. Dock180^{WT}, but not Dock180^{Y1811F}, was phosphorylated by Src (Figure 6E). Next, we performed a reconstitution assay for nucleotide-free Rac binding (22, 23). In the absence of the recombinant Src, when immunoprecipitated Dock180^{WT} or Dock180^{Y1811F} was dephosphorylated by a protein tyrosine phosphatase (PTP), minimal Dock180-Rac1 interaction was seen. However, when a recombinant Src was added, substantial p-Dock180^{WT}, but not p-Dock180^{Y1811F}, was induced, accompanied with an increase in association of Dock180 with Rac1 (Figure 6F). Finally, we knocked down endogenous Src using 2 separate shRNAs (shRNA4 and shRNA5) in LN444/PDGF-A/shDock180 cells with or without reexpression of Dock180^{WT*} or Dock180^{Y1811F*} (Figure 6G). p-Dock180^{Y1811} and Rac1 activation were observed in LN444/PDGF-A/shControl or Dock180^{WT*}-reexpressing cells. However, effective depletion of Src markedly decreased PDGF-A–induced p-Y of Dock180^{WT*} and Rac1 activity in LN444/PDGF-A/shControl and Dock180^{WT*}-restored cells, but had no effect in vector or Dock180^{Y1811F*} cells. As a result, knockdown of Src also inhibited PDGF-A stimulation of cell migration in the control and Dock180^{WT*}-restored cells (Figure 6H). Taken together, these data indicate that Src mediates PDGFRα stimulation of glioma cell migration through specific p-Y of Dock180^{Y1811} and activation of Rac1.

PDGF-A–induced association of Dock180 with PDGFRα is necessary for cell migration. We sought to determine whether endogenous Dock180 also associates with PDGFRα in glioma cells by separately treating SNB19, LN444, and LN443 cells with PDGF-A. Treatment with PDGF-A induced an association of Dock180 with PDGFRα in all 3 cell lines (Figure 7A). To identify which region or domain in Dock180 mediates its association with PDGFRα, we generated several deletion mutants lacking various functional binding domains (Figure 3B and Figure 7B). When these Dock180 deletion mutants were separately cotransfected with PDGFRα$^{\Delta 8,9}$ into HEK293T cells, all Dock180 deletion mutants — as well as a short fragment of Dock180, 1–159 mutant — were able to interact with CA PDGFRα$^{\Delta 8,9}$ (Figure 7, C and D). This suggests that the N-terminal region of aa residues 1–159 of Dock180 protein is involved in its association with activated PDGFRα. To confirm this, we coexpressed PDGFRα$^{\Delta 8,9}$ with a Flag-tagged Dock180 deletion mutant that lacks its N-terminal 1–159 aa residues (Dock180$^{\Delta 160}$) in HEK293T cells and found that the induced Dock180 association with PDGFRα$^{\Delta 8,9}$ was abrogated in cells (Figure 7E), whereas the Dock180^{Y1811F} mutant did not affect Dock180 association with PDGFRα$^{\Delta 8,9}$ (Supplemental Figure 8). To further examine whether this association affects PDGF-A stimulation of p-Y of Dock180 and glioma cell migration, we used LN444/PDGF-A/shDock180-2 cells, in which PDGFRα was activated by PDGF-A expression and endogenous Dock180 was stably depleted (Figure 2A). When a shRNA-resistant Dock180^{WT*} or a shRNA-resistant Dock180$^{\Delta 160*}$ mutant were separately reexpressed, Dock180^{WT*} restored PDGF-A–induced association of Dock180 and ELMO1 with WT PDGFRα and activation of Rac1, whereas Dock180$^{\Delta 160*}$ markedly inhibited its association with PDGFRα and ELMO1 as well as Rac1 activation (Figure 7F). Furthermore, restoration of Dock180^{WT*} enhanced PDGF-A–stimulated LN444/PDGF-A/shDock180-2 cell migration, whereas reexpression of the Dock180$^{\Delta 160*}$ mutant was unable to render the cells responsive to PDGF-A stimulation of cell migration (Figure 7G). Finally, reexpression of a shRNA-resistant Dock180$^{\Delta 160\text{-}Y1811F*}$ mutant (which lacks both the N-terminal 1–159 aa residues and the Y1811 phosphorylation site) attenuated PDGF-A stimulation of Rac1 activities and had an additive effect on reducing cell migration compared with that caused by individual mutations (Figure 7H). Together, these results demonstrated that the N-terminal region of Dock180 (aa residues 1–159) formed a complex with PDGFRα and ELMO1 and modulated PDGF-A–stimulated glioma cell migration without affecting the induced p-Y of Dock180.

Src-dependent p-Dock180^{Y1811} is important for PDGF-A–induced Dock180 association with p130^{Cas} and CrkII; activation of Akt, Erk1/2, and Rac1; and cell migration of primary GBM cells with PDGFRα amplification. To determine whether Src-dependent p-Y of Dock180^{Y1811} is required for Rac1 activation and cell migration in primary GBM cells with PDGFRα overexpression, we used primary GBM5 (*PDGFRA* gene amplification), GBM6 (*EGFR* gene amplification and EGFRvIII overexpression), and GBM14 (no *PDGFRA* or *EGFR* gene amplification) cells (Supplemental Figure 1 and refs. 17, 24). PDGF-A stimulation of primary GBM5 cells with PDGFRα overexpression increased p-Y of Dock180^{Y1811} and Rac1 activities compared with GBM6 and GBM14 cells (Figure 8A). Consistent with our results in Figure 4A, GBM6 cells with EGFRvIII overexpression minimally increased p-Y of Dock180^{Y1811} and increased Rac1 activities with or without PDGF-A stimulation. PDGFRα stimulation also promoted the association among Dock180, p130^{Cas}, CrkII, p-Akt, p-Erk1/2, and Rac1 activities in GBM5 cells, whereas AG1296, PP2, and SU6656 attenuated PDGF-A–induced p-Y of Dock180^{Y1811} and

the association of Dock180, p130^{Cas}, CrkII, p-Akt, p-Erk1/2, Rac1 activities, and cell migration of GBM5 cells (Figure 8, B and D). To further define this signaling, we transiently transfected GBM5 cells with a Dock180 siRNA pool or control siRNA. Knockdown of Dock180 also inhibited PDGF-A stimulation of these biochemical and cellular behaviors in GBM5 cells (Figure 8, C and D). Therefore, these results recapitulated our in vitro and in vivo observations in LN443 and LN444 cells, which further suggests that Src-dependent p-Dock180^{Y1811} is critical for PDGFRα-stimulated Dock180 association with p130^{Cas}, CrkII, p-Akt, p-Erk1/2, Rac1 activities, and cell migration in glioma cells.

p-Dock180^{Y1811} is present with PDGFRα and p-Src^{Y418} in human clinical glioma specimens. Based on accumulating evidence supporting an important function of p-Dock180^{Y1811} in PDGFRα-stimulated glioma tumorigenesis, we sought clinical evidence for a link among p-Dock180^{Y1811}, PDGFRα, and active Src. We immunostained a total of 134 clinical glioma tumor samples using an anti-PDGFRα antibody. PDGFRα proteins were detected in 3 of 26 WHO grade II gliomas (11.5%), 6 of 30 WHO grade III gliomas (20%), and 24 of 78 GBM specimens (30.8%), similar to previously reported frequencies (4, 6). Subsequently, we performed IHC analyses of these PDGFRα-expressing GBM specimens using anti-p-Src^{Y418} and our specific anti-p-Dock180^{Y1811} antibodies. PDGFRα protein was detected in both invasive and central regions in the GBM tumors and in WHO grade II and III tumors (Figure 9, A–F, Supplemental Figures 9 and 10, and data not shown). Notably, both p-Src^{Y418} and p-Dock180^{Y1811} were also expressed in the majority of PDGFRα-positive tumor cells in invasive and central regions of clinical glioma specimens (Figure 9, B, C, E, and F, Supplemental Figure 10, B, C, E, and F, and Supplemental Table 2). In contrast, minimal expression of PDGFRα, p-Src^{Y418}, and p-Dock180^{Y1811} was found in normal brain and WHO grade I glioma specimens (Supplemental Figure 11 and data not shown). Spearman's rank correlation analysis of the expression of PDGFRα and p-Dock180^{Y1811} in clinical glioma specimens by IHC staining corroborated the correlation coefficient between border and border areas ($r^2 = 0.9000$; $P < 0.05$), center and center regions ($r^2 = 0.9000$; $P < 0.05$), and invasion and invasion areas ($r^2 = 0.8721$; $P < 0.05$) (Supplemental Tables 3 and 4).

To further validate these findings, we examined expression of PDGFRα, p-Src^{Y418}, and p-Dock180^{Y1811} by IB analyses in tumor lysates from a separate and independent cohort of 38 clinical GBM specimens. PDGFRα was overexpressed in 4 GBMs (tumors 4, 13, 14, and 30), and PDGFRα protein was detected at moderate to high levels in another 11 tumors (Figure 9G). Dock180 was detected at high levels in 25 of these 38 tumors, and p-Src^{Y418} and phosphorylated p21-activated kinase 1/2 (p-PAK1/2; activated by binding to p21-GTPases, including Rac1) were found in all tumors at different levels. Interestingly, p-Dock180^{Y1811} was coexpressed with p-Src^{Y418} and p-PAK1/2 in 8 PDGFRα-expressing GBMs (Figure 9G), which suggested activation of Src/Dock180/Rac1 signaling in these PDGFRα-expressing GBMs. Kaplan-Meier analysis showed that patients with high levels of both PDGFRα and p-Dock180^{Y1811} had significantly shorter overall survival compared with those with low PDGFRα and p-Dock180^{Y1811} (Figure 9, H and I). Finally, we searched for p-Dock180^{Y1811} in proteomic studies of p-Y proteins in human cancers and found that p-Dock180^{Y1811} has previously been detected in clinical specimens and cell lines of various types of human cancers, including gliomas, lung, breast, bladder, ovarian, oropharyngeal, and nonmelanoma skin cancers (http://www.phosphosite.org and ref. 25). Taken together, these data suggest that Dock180 is found phosphorylated at its Y1811 site, and p-Dock180^{Y1811} is coexpressed with PDGFRα and p-Src^{Y418} in clinical human glioma specimens and could be a clinically useful marker in the diagnosis and assessment of outcome in GBMs with PDGFRα overexpression.

Discussion

Here we report a mechanism by which Rac1, a key modulator of cell motility and growth, is activated by its GEF, Dock180, in PDGFRα-promoted glioma tumorigenesis (Figure 10). We found that Dock180 was not only required for PDGFRα-promoted glioma cell growth, survival, and invasion in vitro and in vivo, but was also specifically p-Y at Y1811 in an Src-dependent manner. p-Dock180^{Y1811} mediated PDGFRα stimulation of glioma tumorigenesis through association of Dock180 with CrkII and p130^{Cas} and activation of Rac1. Additionally, Dock180 was associated with the PDGFRα receptor itself upon PDGF-A stimulation, and, without affecting induced p-Dock180^{Y1811}, disruption of Dock180 association with PDGFRα impeded PDGFRα-promoted glioma cell migration. Furthermore, p-Dock180^{Y1811} and p-Src^{Y418} were coexpressed with PDGFRα in clinical glioma specimens, and p-Dock180^{Y1811} was detected in several types of human cancers, including gliomas. Additionally, expression of p-Dock180^{Y1811} and PDGFRα correlated with a very poor clinical prognosis in patients with gliomas. Taken together, our results suggest a critical role of activation of p-Dock180^{Y1811}/Rac1 signaling in promoting cancer tumorigenesis.

Genetic studies have established a pathway of Dock180/CrkII/Rac in *C. elegans* (11) and placed Dock180/Rac1 downstream of PVR (the homolog of PDGFR/VEGFR) in *Drosophila* (14, 26). In the present study, we further established that PDGF-A stimulation of PDGFRα induced Src-dependent p-Y at Dock180^{Y1811}, leading to the formation of the Dock180/CrkII/p130^{Cas} complex and activation of Rac1 signaling and thereby promoting glioma cell growth, survival, and invasion (Figure 10). Since Rac1 is a direct downstream target of Dock180 (11) and mediates cancer cell growth, survival, and motility (10, 15, 27), inhibition of Dock180 by siRNA knockdown or reversion with Dock180^{Y1811F*} abrogated PDGFRα-stimulated Rac1 activity and tumorigenic behaviors of glioma cells in vitro and in vivo. Moreover, inhibition of Dock180 attenuated PDGFRα activation of p-Erk1/2, but with less reduction of p-Akt. We recently demonstrated that in glioblastomas deficient in *Ink4a/Arf*, overexpressed PDGFRα promotes tumorigenesis through the PI3K/Akt/mTOR-mediated pathway regulated by SHP-2 (8). Since both PDGFRα/PI3K signaling and PDGFRα/Src/Dock180/Rac1 signaling stimulate p-Akt, inhibition of Dock180 only partially reduced p-Akt, but attenuated PDGFRα-promoted survival and growth of glioma cells. On the other hand, inhibition of PI3K by LY294002 did not affect PDGF-A–induced p-Y of PDGFRα and p-Y of Dock180, but abrogated PDGF-A stimulation of Rac1 activities and cell migration, corroborating a recent study showing that PI3K is upstream of Rac1 in PDGFRα-induced cell migration (21). Additionally, the requirement for both PI3K/Akt/SHP-2/mTOR and Src/Dock180/Rac1 signaling in PDGFRα-promoted glioma tumorigenesis (ref. 8 and the present study) recapitulates the heterogeneity of glioblastomas that engenders their malignancy through multiple pathways. This hypothesis is further supported by our data showing that activated PAK1/2 (p-PAK1/2) and active Src (p-Src^{Y418}) were found in each of the 38 clinical GBM specimens analyzed, whereas active Dock180 (p-Dock180^{Y1811}) was only observed in 10 of them. PAK1/2 is activated by several p21-GTPases, including Rac1 and Cdc42 (9). We also made a similar observation in our IHC, studies in which p-Dock180^{Y1811} was absent in a number of glioma samples that

express PDGFRα and/or p-Src^{Y418}. Since PDGFRα and p-Src^{Y418} are activated in glioblastomas (2, 3, 28), GBMs that lack p-Dock180^{Y1811} might use alternative signaling pathways for their tumorigenesis. Taken together, our results not only corroborated with genetic studies showing that Dock180/Rac mediates cell migration induced by PDGFR (PVR in *Drosophila*) (14), but also integrate PDGFRα activation of Src into p-Dock180^{Y1811}/Rac1–promoted glioma cell growth, survival, and invasion (Figure 10).

Dock180 was identified as a binding protein for c-Crk through its C-terminal PxxP region (29). The PxxP domain–mediated formation of a Dock180/CrkII/p130^{Cas} complex is required for integrin stimulation of Rac1 and cell motility (11). Importantly, Y1811 is located within this PxxP domain (Figure 3B), which is highly conserved in Dock180 from opossum to humans, but not in other members of the Dock family (Figure 3F and Supplemental Figure 2). Since Dock180 activity is regulated by a conformational change upon ELMO1 association (11), it is possible that the PDGFRα-induced p-Dock180^{Y1811} at its C-terminal PxxP domain and formation of the Dock180/CrkII/p130^{Cas} complex caused a further conformation change, resulting in increased Dock180 binding to Rac1 and Rac1 activation. This provides a rationale for the observed biological and biochemical consequences of the specific p-Dock180^{Y1811} in PDGFRα-stimulated gliomagenesis. Furthermore, overexpression of PDGFRα in clinical GBMs (4), co-overexpression of p-Dock180^{Y1811} with PDGFRα and p-Src^{Y418} in clinical glioma specimens, and the occurrence of p-Dock180^{Y1811} in several types of human cancers (ref. 25 and http://www.phosphosite.org) suggest that p-Dock180^{Y1811} could be specifically responsible for the activation of Rac1 that promotes tumorigenesis of human cancers.

PDGF induces Src association with PDGFRα at a specific p-Y docking site in the receptor (30). Moreover, upon stimulation of RTKs, Src induces p-Y of several GEFs, such as Vav2 (10), which suggests that Src-dependent p-Y of GEFs could be a mechanism in RTK-promoted tumorigenesis. Our data support this hypothesis. In contrast to a previous report of p-Y of ELMO1 by Src family kinase Hck (31), we did not detect p-Y of ELMO1 upon PDGFRα activation. However, p-Dock180^{Y1811} was markedly induced in PDGF-A–stimulated glioma cells and primary GBM5 cells with PDGFRα overexpression, and inhibition of Src impaired PDGFRα-induced p-Dock180^{Y1811}. In silico analyses identified Y1811 and other potential p-Y sites in Dock180 as Src substrate sites. Our data validated Y1811 as a PDGFRα-induced Src p-Y site. Additionally, there was a minor p-Y site of Dock180 that was induced by PDGFRα activation (Figure 3E), but was not affected by Src inhibitors (Figure 6A), suggestive of a Src-independent p-Y of Dock180 not involved in PDGFRα-stimulated cell migration (Figure 6B). Based on these data, it would be predicted that Src family kinase inhibitors such as Dasatinib or AZD0530 (20) could be effective to inhibit PDGFRα-promoted glioma tumorigenesis in the brains of animals. However, caution is in order with this idea, since the Src family kinase inhibitors PP2 and SU6656 were previously shown to have minimal or moderate impact on PDGFRα-stimulated anchorage-independent growth of human glioma cells in vitro (8).

Multiple Rho GEFs interact with RTKs through various functional domains, affecting their GEF activities (12). We showed that PDGF-A induced an association of Dock180 with PDGFRα through its N-terminal domain (1–159 aa residues), which was critical for PDGFRα-stimulated Rac1 activity and glioma cell migration. The interaction region of Dock180 contains a SH3 domain that binds to ELMO1. Reexpression of shRNA-resistant Dock180$^{\Delta 160*}$, but not Dock180^{WT*}, in LN444/PDGF-A/shDock180 cells resulted in loss of interaction among Dock180$^{\Delta 160*}$, PDGFRα, and ELMO1, loss of Rac1 activity, and decreased glioma cell migration without affecting induction of p-Y of Dock180. Additionally, a double Dock180$^{\Delta 160\text{-}Y1811F*}$ mutant showed an additive effect on the inhibition of PDGFRα stimulation. Our data could explain the previous observation that overexpression of Dock180 lacking the DHR-1 domain — which is a PtdIns(3,4,5)P3-binding domain — leads to activation of Rac1 (32) and does not require ELMO1 for this activity (11). We speculate that PDGF-A induces association of Dock180 with PDGFRα through the N-terminal region (1–159 aa residues) of Dock180, which probably is adjacent to or overlaps with the SH3 domain that binds to ELMO1, thereby opening the inhibitory folding configuration of Dock180 in unstimulated cells (11). Interaction of Dock180 with PDGFRα could additionally target Dock180 to the membrane in synergy with the DHR-1 domain, inducing formation of the Dock180/CrkII/p130^{Cas} complex and stimulating Rac1 activities and cell motility (11). These data also support the hypothesis that DHR-1 plays a role in dynamic membrane targeting of the Rho GEF activity of Dock180 in PDGFRα-activated cells (33). On the other hand, we found that association of Dock180 to PDGFRα was independent of Src-induced p-Dock180^{Y1811}, since the Dock180^{Y1811F} mutant was still able to bind to PDGFRα upon PDGF-A stimulation. Moreover, disruption of Dock180 binding to PDGFRα, a single Dock180^{Y1811F} mutant, or a double Dock180$^{\Delta 160\text{-}Y1811F*}$ mutant abrogated PDGF-A activation of Rac1 and cell motility. The requirement of these 2 separate mechanisms fits well with a hypothetical 2-step model of bipartite GEF activation (11). Namely, in addition to association with ELMO1, PDGF-A–induced binding of Dock180 to PDGFRα targets Dock180 to the membrane, thereby facilitating interaction of ELMO1 and Dock180 with nucleotide-free Rac1. Since Y1811 is located farther away from the N-terminal SH3 domain of Dock180 and may not involve in the interaction of Dock180 with Rac1, it is possible that the PxxP domain with unphosphorylated Dock180^{Y1811} could hinder the loading of GTP into nucleotide-free Rac1. Src-induced p-Dock180^{Y1811} and formation of the Dock180/CrkII/p130^{Cas} complex caused a further conformation change of Dock180, thereby allowing GTP loading to nucleotide-free Rac1 and resulting in activation of Rac1 signaling and various cellular functions. However, this hypothesis warrants further investigation.

In summary, our data reveal a mechanism by which PDGFRα stimulates glioma tumorigenesis through PDGFRα-induced Src-dependent p-Y of Dock180^{Y1811} as well as Dock180 association with activated PDGFRα, thereby activating the Dock180/CrkII/p130^{Cas}/Rac1 pathway. This is underscored by coexpression of p-Dock180^{Y1811} and p-Src^{Y418} with overexpressed PDGFRα in clinical glioma specimens and a notable association with very poor patient survival. It also fits well with the occurrence of p-Dock180^{Y1811} that is detected by proteomic analysis in various types of human cancers, including gliomas. Since p-Y of Rho GEFs is a common mechanism affecting GEF activity, and Src is aberrantly activated in human cancers, including gliomas, our study suggests that the PDGFRα/Src/p-Dock180^{Y1811}/Rac1 signaling axis could represent a novel and attractive therapeutic target for glioblastomas and other types of human cancer that overexpress PDGFRα.

Methods

Cell lines and reagents. HEK293T, glioma U87, U251, U373, and T98G cells (all from ATCC); SNB19, LNZ308, LN18, LN235, LN319, LN443, and LN444 cells; and unaltered primary human GBM cells were cultured as previously described (15, 24, 34). Rabbit polyclonal antibodies

to p-Dock180^{Y1811} were produced by immunizing animals with a synthetic phosphopeptide corresponding to residues surrounding human Dock180^{Y1811}. The antibodies were then affinity purified. YOP PTP was from Enzo Life Science; recombinant Src protein was from Active Motif; and lentivirus-encoded Src shRNAs were from The Broad Institute. Flag-Dock180 was provided by M. Matsuda (Kyoto University, Kyoto, Japan); PDGFRα$^{\Delta 8,9}$ by I. Clarke (University of Toronto, Toronto, Ontario, Canada); PDGF-A and PDGFRα by C.-H. Heldin (Uppsala University, Uppsala, Sweden); CrkII by R. Birge (UMDNJ–New Jersey Medical School, Newark, New Jersey, USA); Src-WT, -KD, and -CA by S. Courtneidge (Sanford-Burnham Medical Research Institute, La Jolla, California, USA); pMXI-*gfp* by R. Pieper (UCSF, San Francisco, California, USA); and SNB19 cells by Y. Zhou (UCI, Irwin, California, USA).

Purification of recombinant proteins. Protein purifications were performed at 4°C. $(His)_6$-tagged Dock180^{WT} and Dock180^{Y1811F} proteins were purified from serum-starved HEK293T cells transiently transfected with pcDNA3-$(His)_6$-Dock180^{WT} and -Dock180^{Y1811F}, respectively. Cells were lysed and sonicated. The lysates were centrifuged, and the supernatants were loaded onto a Ni^+-NTA column in 10 mM imidazole buffer. After washing 2×, Ni^+-bound proteins were eluted with a 500 mM imidazole buffer followed by dialysis against PBS. The purified recombinant Dock180 proteins were examined by Coomassie blue staining and IB analyses. The aliquots were stored at 80°C until use.

In vitro Src p-Y and Rac1/Dock180 binding assays. 500 ng purified recombinant Dock180^{WT} or Dock180^{Y1811F} proteins were incubated with 200 μM cold ATP in the presence or absence of 100 ng recombinant active Src kinase (Active Motif) in 30 μl reaction buffer (60 mM Hepes-NaOH, pH 7.5, 3 mM $MnCl_2$, 3 mM $MgCl_2$, 3 M Na_3VO_4, 1.2 mM DTT, 1.5 μg PEG 20,000) at 30°C for 30 minutes and then chilled on ice. The reaction products were mixed with an equal volume of 2× SDS sample buffer and p-Dock180^{Y1811}, then examined by IB analyses using the specific anti-p-Dock180^{Y1811} antibody.

The effect of Src-induced p-Dock180^{Y1811} on Rac1 binding was determined as previously described (22, 23). Briefly, Flag-tagged Dock180^{WT} or Dock180^{Y1811F} cDNAs were transfected into HEK293T cells for 48 hours. Cells were then lysed, and Flag-tagged Dock180^{WT} or Dock-180^{Y1811F} proteins were subjected to IP using an anti-Flag antibody. The precipitates were then treated with 15 μM of a recombinant YOP PTP at 30°C for 1 hour in 1× YOP reaction buffer (50 mM citrate, pH 6.0, 100 mM NaCl, 1 mM EDTA, and 1 mM DTT) containing 1 mg/ml BSA, washed 3× with PBS, and incubated with or without a recombinant Src kinase at 30°C for 30 minutes. The treated mixtures were washed again and incubated with total lysates prepared from HEK293T cells that were transfected with a EGFP-Rac1 cDNA with 10 mM EDTA at 4°C for 90 minutes. The reaction products were mixed with an equal volume of IP buffer or 2× SDS sample buffer and examined by IP and IB analyses.

IHC and IB analyses of human and mouse glioma specimens. In total, 134 primary human glioma specimens were collected from 2001 to 2008 at Saitama Medical University and Kyorin University. Specimens were examined and diagnosed by a neuropathologist, then analyzed by IHC using an anti-PDGFRα antibody (diluted 1:20) as we previously described (15). IHC analyses were further performed on 33 specimens that were positive for PDGFRα expression and 9 samples that were negative for PDGFRα expression using specific anti-p-Dock180^{Y1811} and anti-p-Src^{Y418} antibodies (diluted 1:20 and 1:10, respectively). Mouse brain sections with various tumors were analyzed by IHC using an anti-Ki-67 antibody (diluted 1:200) or a TUNEL staining kit. Images were captured using a microscope equipped with a digital camera. 5 random images per section of mouse brains were obtained, and percentage of Ki-67- or TUNEL-positive cells was quantified and statistically analyzed as previously described (8).

A separate and independent cohort of a total of 38 snap-frozen WHO grade IV GBM tissue samples were obtained from the University of Pittsburgh Medical Center Tissue Bank. These tissue samples were neurological specimens discarded as excess tissues and collected and banked by the Tissue Bank at the University of Pittsburgh; tumors were examined and diagnosed by a neuropathologist. The small frozen fragments of tumor tissues (0.07–0.9 g) were processed and analyzed by IB assays (8).

Gene knockdown by siRNA or shRNA; mutagenesis, IP, IB, cell proliferation, and viability assays; in vitro cell migration and Rac1 activation assays; mouse glioma xenografts; gene expression analysis; and quantitative PCR analysis for gene copy numbers. See Supplemental Methods.

Statistics. GraphPad Prism version 4.00 for Windows was used to perform 1-way ANOVA with Newman-Keuls post-test or paired 2-tailed Student's *t* test and χ^2 test as previously described (15). A *P* value of 0.05 or less was considered statistically significant.

Study approval. Studies using human tissues were reviewed and approved by the Institutional Review Board involving Human Subjects of the University of Pittsburgh. The specimens were deidentified human tissues; thus, no informed consent was required.

Acknowledgments

The authors thank M. Matsuda, I. Clarke, C.-H. Heldin, R. Birge, S. Courtneidge, R. Pieper, and Y. Zhou for providing reagents, as well as T. Hirose (Saitama Medical University, Moroyama, Japan) for examining tumor specimens. This work was supported by NIH grants CA102011 and CA130966 to S.-Y. Cheng; by a Brain Cancer Research Award from James S. McDonnell Foundation to B. Hu; by a grant with the Pennsylvania Department of Health and Innovative Research Scholar Awards of the Hillman Foundation to S.-Y. Cheng and B. Hu; by NIH grant CA102583 to K. Vuori; by NIH grant HL070561, National Basic Research Program of China grant 2011CB964801, Outstanding Young Scholar Award from the National Natural Science Foundation of China 30825017, Tianjin International Cooperation Science Foundation grant 09ZCZDSF03800, and a Scholar Award from the Leukemia and Lymphoma Society to T. Cheng; by Mayo Brain Tumor SPORE grant CA108961 to J.N. Sarkaria; by an award from the Goldhirsh Foundation to F. Furnari; and by NIH grant P01-CA95616 to W.K. Cavenee and F. Furnari. W.K. Cavenee is a fellow of the National Foundation for Cancer Research. This project used the shared facilities at the University of Pittsburgh Cancer Institute that were supported in part by NIH grant P30CA047904.

Received for publication April 21, 2011, and accepted in revised form October 5, 2011.

Address correspondence to: Bo Hu, University of Pittsburgh Cancer Institute and Department of Medicine, 5117 Centre Avenue, 2.26, Pittsburgh, Pennsylvania 15213, USA. Phone: 412.623.7791; Fax: 412.623.4840; E-mail: hub@upmc.edu. Or to: Shi-Yuan Cheng, University of Pittsburgh Cancer Institute and Department of Pathology, 5117 Centre Avenue, 2.26f, Pittsburgh, Pennsylvania 15213, USA. Phone: 412.623.3261; Fax: 412.623.4840; E-mail: chengs@upmc.edu.

Kun-Wei Liu's present address is: Tumor Development Program, Sanford-Burnham Medical Research Institute, La Jolla, California, USA.

Tim Fenton's present address is: Laboratory of Viral Oncology, UCL Cancer Institute, London, United Kingdom.

1. Wen PY, Kesari S. Malignant gliomas in adults. *N Engl J Med.* 2008;359(5):492–507.
2. Furnari FB, et al. Malignant astrocytic glioma: genetics, biology, and paths to treatment. *Genes Dev.* 2007;21(21):2683–2710.
3. Van Meir EG, Hadjipanayis CG, Norden AD, Shu HK, Wen PY, Olson JJ. Exciting new advances in neuro-oncology: the avenue to a cure for malignant glioma. *CA Cancer J Clin.* 2010;60(3):166–193.
4. Cancer Genome Atlas Research Network. Comprehensive genomic characterization defines human glioblastoma genes and core pathways. *Nature.* 2008;455(7216):1061–1068.
5. Parsons DW, et al. An integrated genomic analysis of human glioblastoma multiforme. *Science.* 2008;321(5897):1807–1812.
6. Verhaak RG, et al. Integrated genomic analysis identifies clinically relevant subtypes of glioblastoma characterized by abnormalities in PDGFRA, IDH1, EGFR, and NF1. *Cancer Cell.* 2010;17(1):98–110.
7. Shih AH, Holland EC. Platelet-derived growth factor (PDGF) and glial tumorigenesis. *Cancer Lett.* 2006;232(2):139–147.
8. Liu KW, et al. SHP-2/PTPN11 mediates gliomagenesis driven by PDGFRA and INK4A/ARF aberrations in mice and humans. *J Clin Invest.* 2011; 121(3):905–917.
9. Burridge K, Wennerberg K. Rho and Rac take center stage. *Cell.* 2004;116(2):167–179.
10. Rossman KL, Der CJ, Sondek J. GEF means go: turning on RHO GTPases with guanine nucleotide-exchange factors. *Nat Rev Mol Cell Biol.* 2005; 6(2):167–180.
11. Cote JF, Vuori K. GEF what? Dock180 and related proteins help Rac to polarize cells in new ways. *Trends Cell Biol.* 2007;17(8):383–393.
12. Schiller MR. Coupling receptor tyrosine kinases to Rho GTPases--GEFs what's the link. *Cell Signal.* 2006;18(11):1834–1843.
13. Duchek P, Somogyi K, Jekely G, Beccari S, Rorth P. Guidance of cell migration by the Drosophila PDGF/VEGF receptor. *Cell.* 2001;107(1):17–26.
14. Bianco A, et al. Two distinct modes of guidance signalling during collective migration of border cells. *Nature.* 2007;448(7151):362–365.
15. Jarzynka MJ, et al. ELMO1 and Dock180, a bipartite Rac1 guanine nucleotide exchange factor, promote human glioma cell invasion. *Cancer Res.* 2007;67(15):7203–7211.
16. Martinho O, et al. Expression, mutation and copy number analysis of platelet-derived growth factor receptor A (PDGFRA) and its ligand PDGFA in gliomas. *Br J Cancer.* 2009;101(6):973–982.
17. Giannini C, et al. Patient tumor EGFR and PDGFRA gene amplifications retained in an invasive intracranial xenograft model of glioblastoma multiforme. *Neuro-oncol.* 2005;7(2):164–176.
18. Kovalenko M, et al. Selective platelet-derived growth factor receptor kinase blockers reverse sis-transformation. *Cancer Res.* 1994;54(23):6106–6114.
19. Ozawa T, et al. PDGFRA gene rearrangements are frequent genetic events in PDGFRA-amplified glioblastomas. *Genes Dev.* 2010;24(19):2205–2218.
20. Kim LC, Song L, Haura EB. Src kinases as therapeutic targets for cancer. *Nat Rev Clin Oncol.* 2009; 6(10):587–595.
21. Pickett EA, Olsen GS, Tallquist MD. Disruption of PDGFRalpha-initiated PI3K activation and migration of somite derivatives leads to spina bifida. *Development.* 2008;135(3):589–598.
22. Brugnera E, et al. Unconventional Rac-GEF activity is mediated through the Dock180-ELMO complex. *Nat Cell Biol.* 2002;4(8):574–582.
23. Kang S, et al. FGFR3 activates RSK2 to mediate hematopoietic transformation through tyrosine phosphorylation of RSK2 and activation of the MEK/ERK pathway. *Cancer Cell.* 2007;12(3):201–214.
24. Yiin JJ, et al. ZD6474, a multitargeted inhibitor for receptor tyrosine kinases, suppresses growth of gliomas expressing an epidermal growth factor receptor mutant, EGFRvIII, in the brain. *Mol Cancer Ther.* 2010;9(4):929–941.
25. Rikova K, et al. Global survey of phosphotyrosine signaling identifies oncogenic kinases in lung cancer. *Cell.* 2007;131(6):1190–1203.
26. Haralalka S, Shelton C, Cartwright HN, Katzfey E, Janzen E, Abmayr SM. Asymmetric Mbc, active Rac1 and F-actin foci in the fusion-competent myoblasts during myoblast fusion in Drosophila. *Development.* 2011;138(8):1551–1562.
27. Senger DL, et al. Suppression of Rac activity induces apoptosis of human glioma cells but not normal human astrocytes. *Cancer Res.* 2002; 62(7):2131–2140.
28. Kleber S, et al. Yes and PI3K bind CD95 to signal invasion of glioblastoma. *Cancer Cell.* 2008; 13(3):235–248.
29. Hasegawa H, et al. DOCK180, a major CRK-binding protein, alters cell morphology upon translocation to the cell membrane. *Mol Cell Biol.* 1996; 16(4):1770–1776.
30. Tallquist M, Kazlauskas A. PDGF signaling in cells and mice. *Cytokine Growth Factor Rev.* 2004; 15(4):205–213.
31. Yokoyama N, et al. Identification of tyrosine residues on ELMO1 that are phosphorylated by the Src-family kinase Hck. *Biochemistry.* 2005; 44(24):8841–8849.
32. Komander D, et al. An alpha-helical extension of the ELMO1 pleckstrin homology domain mediates direct interaction to DOCK180 and is critical in Rac signaling. *Mol Biol Cell.* 2008;19(11):4837–4851.
33. Premkumar L, et al. Structural basis of membrane targeting by the Dock180 family of Rho family guanine exchange factors (Rho-GEFs). *J Biol Chem.* 2010;285(17):13211–13222.
34. Ishii N, et al. Frequent co-alterations of TP53, p16/CDKN2A, p14ARF, PTEN tumor suppressor genes in human glioma cell lines. *Brain Pathol.* 1999;9(3):469–479.

J Neurooncol (2012) 107:147–153
DOI 10.1007/s11060-011-0721-3

CLINICAL STUDY – PATIENT STUDY

O^6-methylguanine-DNA methyltransferase promoter methylation in 45 primary central nervous system lymphomas: quantitative assessment of methylation and response to temozolomide treatment

Jun-ichi Adachi · Kazuhiko Mishima · Kenji Wakiya · Tomonari Suzuki · Kohei Fukuoka · Takaaki Yanagisawa · Masao Matsutani · Atsushi Sasaki · Ryo Nishikawa

Received: 13 June 2011 / Accepted: 17 September 2011 / Published online: 4 October 2011

Abstract Favorable responses to temozolomide chemotherapy have recently been reported in primary central nervous system lymphoma (PCNSL) patients who are refractory to high-dose methotrexate therapy. The gene encoding the DNA repair enzyme O^6-methylguanine-DNA methyltransferase (MGMT) is transcriptionally silenced by promoter methylation in several human tumors, including gliomas and systemic lymphomas. *MGMT* promoter methylation is also a prognostic marker in glioblastoma patients treated with temozolomide. To validate temozolomide treatment in PCNSL, we applied methylation-sensitive high resolution melting (MS-HRM) analysis to quantitate *MGMT* methylation in PCNSL. *MGMT* promoter methylation was detected in tumors from 23 (51%) of 45 PCNSL patients, 11 of which were considered to have high (more than 70.0%) methylation status. Of the five recurrent PCNSLs treated with temozolomide, four cases responded, with three achieving complete response and one, a partial response. All four responsive PCNSLs had methylated *MGMT* promoters, whereas the non-responsive recurrent PCNSL did not. Thus, the use of quantitative MS-HRM analysis for the detection of *MGMT* promoter methylation has been suggested in PCNSL for the first time. The assay allows rapid and high-throughput evaluation of the *MGMT* methylation status, and seems to be promising in clinical settings. *MGMT* promoter methylation may become a useful marker for predicting the response of PCNSLs to temozolomide.

Keywords Primary central nervous system lymphoma · MGMT · Temozolomide · Chemotherapy

J. Adachi (✉) · K. Mishima · K. Wakiya · T. Suzuki · K. Fukuoka · T. Yanagisawa · M. Matsutani · R. Nishikawa
Department of Neuro-Oncology/Neurosurgery, Comprehensive Cancer Center, Saitama Medical University International Medical Center, 1397-1 Yamane, Hidaka-shi, Saitama 350-1298, Japan
e-mail: jadachi@saitama-med.ac.jp

A. Sasaki
Department of Pathology, Saitama Medical University, 38 Morohongo, Moroyama-machi, Iruma-gun, Saitama 350-0495, Japan

Introduction

Primary central nervous system lymphoma (PCNSL) is characterized by rapid progression, frequent cerebrospinal fluid involvement, and early recurrence [1]. The introduction of combined pre-irradiation high-dose methotrexate (HD-MTX) with radiation therapy has resulted in a median survival time of 33 months [2, 3]. HD-MTX, however, is associated with considerable systemic toxicity affecting renal, cardiac, and hematological function [4]. There are also important limitations of radiation therapy, including an increased risk of late neurotoxicity, especially in elderly patients [5]. Thus, there is a need for an alternative chemotherapy that is both efficient and well-tolerated. Cyclophosphamide–adriamycin–vincristine–prednisolone (CHOP) chemotherapy is the standard chemotherapy for systemic malignant lymphoma, but the drugs do not penetrate the brain effectively and do not improve survival of patients with PCNSL [6, 7]. Temozolomide is an alkylating agent with good cerebrospinal fluid penetration [8], and there have been some reports of temozolomide efficacy with acceptable toxicity in cases of PCNSL [9–12].

Previous studies on glioma and systemic lymphoma associated the presence of the methylated form of the O^6-methylguanine-DNA methyltransferase (*MGMT*) gene

with a more favorable response to alkylating agents [13–15]. MGMT is a DNA repairing enzyme that removes alkyl adducts from the O^6 position of guanine and prevents the cytotoxic, mutagenic, and carcinogenic effects of alkylating agents such as temozolomide [16–19]. It has been demonstrated that silencing of *MGMT* is involved in carcinogenesis in humans [20, 21]. The loss of *MGMT* function in human cancer cells is mainly due to the hypermethylation of CpG islands in the gene's promoter sequence [22, 23]. Therefore, evaluation of the methylation status of the *MGMT* promoter is important to validate temozolomide treatment in PCNSL.

In this study, we applied, for the first time, methylation-sensitive high resolution melting (MS-HRM) analysis to quantify the *MGMT* methylation status in 45 cases of PCNSL. In addition, the *MGMT* methylation level was compared with the clinical response to temozolomide treatment.

Patients and methods

Patients and treatment

We studied 45 patients with newly diagnosed PCNSL between 2002 and 2011. Tumor samples were obtained by surgical resection or biopsy prior to therapy. On the basis of pathological examination, a diagnosis of diffuse large B cell lymphoma was made in all cases. Written informed consent for use of their tissues was obtained from study subjects.

The primary treatment was high-dose methotrexate (HD-MTX)-based chemotherapy in 43 patients, and exclusive radiation therapy (RT) in one patient, and one patient received no adjuvant treatment after surgery. The MTX dose was 1–3.5 g/m^2. MTX was used as a single agent in 15 patients, and was combined with 375 mg/m^2 rituximab in 28 patients. After primary chemotherapy, RT was performed in 32 of 43 cases. The remaining 11 cases were patients older than 65 years, and were treated without RT to avoid cognitive dysfunction due to radiation-induced leukoencephalopathy. We continued HD-MTX-based chemotherapy for these 11 patients until the tumor progressed.

Fourteen patients received oral temozolomide at 150–200 mg/m^2 per day for 5 days every 4 weeks (Table 1). Five (cases 1–5) of 14 cases were treated with temozolomide as salvage chemotherapy upon relapse after standard HD-MTX/radiation therapy. For the remaining nine patients (cases 6–14), temozolomide was used as adjuvant chemotherapy after first-line HD-MTX therapy.

DNA extraction and *MGMT* quantitative methylation assay

Genomic DNA was extracted from fresh frozen (43 of 45 cases) or paraffin-embedded formalin-fixed (2 of 45 cases)

Table 1 Summary of 14 PCNSL patients treated with temozolomide

Case No.	Age at temozolomide treatment (years)/ gender	No. of temozolomide cycles[a]	Maximum response to temozolomide	Duration (months) keeping CR or PR	Therapy prior to temozolomide treatment	Degree of *MGMT* promoter methylation[b]
1	75/M	19	CR	38	M, R, RT	61.7 ± 4.04
2	60/M	3	CR	12	M, R, RT	99.0 ± 1.00
3	47/M	5	PR	7	M, R, RT	72.3 ± 2.52
4	72/M	2	PD		M, R, RT	1.3 ± 1.26
5	50/M	8	CR	7	M, R, ICE, RT	94.3 ± 2.50
6	64/F	2	CR	11	M	7.7 ± 0.58
7	73/F	6	CR	11	M, RT	0.8 ± 0.96
8	70/M	5	CR	21	M, RT	1.5 ± 1.28
9	55/M	4	CR	27	M, R, RT	26.7 ± 0.58
10	57/M	3	CR	24	M, R, RT	1.8 ± 0.96
11	54/M	3	PD		M, R, RT	32.0 ± 1.83
12	62/F	2	CR	24	M, R, RT	0.3 ± 0.50
13	72/M	10	PR	9	M, R, RT	1.0 ± 0.82
14	85/F	9	CR	7	M, R	74.7 ± 0.58

Cases 1–5 were treated with temozolomide as salvage chemotheapy at relapse after standard HD-MTX/radiation therapy. Cases 6–14 were treated with adjuvant temozolomide therapy after first-line HD-MTX therapy

CR complete response; *PR* partial response; *PD* progressive disease

M HD-MTX; *R* rituximab; *ICE* Ifosfamide + Cisplatin + Etoposide; *RT* radiation therapy

[a] Patients received oral temozolomide for 5 days every 4 weeks

[b] Percentage of *MGMT* methylation level in our assay. The mean ± standard deviation is indicated

Table 2 The primers designed to target the promoter sequences of the *MGMT* gene

	Primer sequences 5′–3′
MGMT MS-HRM[a]	F-GCGTTTCGGATATGTTGGGATAGT
	R-CCTACAAAACCACTCGAAACTACCA

[a] Methylation-sensitive high-resolution melting

brain biopsy specimens using the DNeasy Tissue kit (Qiagen, Hilden, Germany) according to the manufacturer's protocol.

We quantified the methylation status of the *MGMT* promoter's CpG-rich region using MS-HRM analysis [24]. Briefly, 500 ng of genomic DNA was treated with sodium bisulfite using the Epitect Bisulfite Kit (Qiagen, Hilden, Germany) according to the manufacturer's instructions. PCR amplification and MS-HRM analysis were carried out sequentially on a LightCycler480 real-time PCR system (Roche Diagnostics, Mannheim, Germany). The primer sets to amplify 18 CpG-rich sites in the *MGMT* promoter were designed according to previous reports (Table 2) [24, 25]. Each PCR run contained 2 μl of bisulfite-converted DNA in a total volume of 20 μl: 2× master mix containing high-resolution melting dye (Roche Diagnostics, Mannheim, Germany), 4 mM Mg^{2+}, and 500 nM of each primer. Cycling conditions were 10 min at 95°C, followed by 45 cycles of denaturation at 95°C for 15 s, annealing at 60°C for 20 s, and extension at 60°C for 20 s. The melting step was 95°C for 1 min, 50°C for 1 min, 72°C for 5 s, and continuous acquisition to 95°C at 30 acquisitions per 1°C. As positive (100% methylated) and negative (0% methylated) controls, we used CpGenome™ Universal Methylated and Unmethylated DNA (Chemicon, Millipore, Billerica, MA), respectively. The duration of the run from the onset of PCR was approximately 80 min. All reactions were performed at least in triplicate.

Methylation-specific polymerase chain reaction (MSP)

Bisulfite-treated DNA was also subjected to MSP assay of *MGMT* promoter methylation in 14 PCNSL patients treated with temozolomide. We developed nested PCR using primers described in Esteller et al. and Palmisano et al. [23, 27]. The first round of PCR was performed to amplify a 289 bp fragment of the *MGMT* gene including a portion of their CpG-rich promoter region. Primer sequences used in the first round amplification are as follows: 5′-GGA TATGTTGGGATAGTT-3′ (sense) and 5′-CCAAAAACC CCAAACCC-3′ (antisence). 5 μl of the first round PCR products was subjected to the second round PCR in which primers specific to methylated or unmethylated template. A 93 bp unmethylated product was amplified using the primers: 5′-TTTGTGTTTTGATGTTTGTAGGTTTTTG T-3′ (sense) and 5′-AACTCC AACACTCTTCCAAA AACAAAACA-3′ (antisense). An 81 bp methylated product was amplified using the following primers: 5′-TTT CGACGTTCGTAGGTTTTCGC-3′ (sense) and 5′-GCAC TCTTCCGAAAACGAAACG-3′ (antisense). The PCR mixture contained 5 μl DNA, 10× PCR Buffer (TaKaRa), 5 nmol each deoxynucleotide, 2.5 pmol of each primer and 0.8 U *Taq* HS (TaKaRa), in a final volume of 50 μl. The first round PCR cycling conditions were as follows: 95°C for 10 min, then denature at 95°C for 30 s, anneal at 52°C for 30 s, extension at 72°C for 30 s for 40 cycles followed by a 10 min final extension. In the second round PCR, annealing temperature was increased to 62°C and all of the cycling times were reduced to 15 s for a total of 34 cycles. An aliquot of 10 μl of the second round PCR was loaded onto a 12.5% polyacrylamide gel, stained with ethidium bromide and visualized under UV illumination.

Results

Melting data collected using the LightCycler480 Instrument can be analyzed by the "Tm (Melting Temperature) calling" algorithm that converts the melting profiles into derivative plots, which allows methylated and unmethylated samples to be distinguished. Products amplified from methylated DNA have a higher Tm due to the presence of CpGs in the amplicon. In contrast, products amplified from unmethylated DNA have a low Tm due to the conversion of unmethylated cytosine to uracil in the bisulfite-modified DNA sample, which results in thymine in the amplicon. If the sample contains a mixture of methylated and unmethylated DNA, two peaks are displayed, as shown in Fig. 1. This assay was able to detect 1.0% methylated DNA over a background of unmethylated DNA. We used the LightCycler480 Gene Scanning Software ver.1.5 to generate standard curves for methylated *MGMT* using serial samples having known ratios of methylated to unmethylated template. The *MGMT* methylation level of an unknown sample could then be estimated from these standard curves. The samples were analyzed at least in triplicates, and we determined the methylation levels from the average value of the experiments. A cut-off value of 4.0% methylated *MGMT* was previously validated by strong correlation of protein expression loss with MGMT promoter methylation [26]. Therefore, samples with an average *MGMT* methylation level of less than 4.0% were defined as unmethylated.

Of the 45 PCNSLs examined by MS-HRM assay, all samples were amplifiable and gave interpretable results. The *MGMT* promoter was methylated in 23 PCNSLs (51%), and was unmethylated in the remaining 22 cases